

INFORMATION TO USERS

This material was produced from a microfilm copy of the original document. While the most advanced technological means to photograph and reproduce this document have been used, the quality is heavily dependent upon the quality of the original submitted.

The following explanation of techniques is provided to help you understand markings or patterns which may appear on this reproduction.

1. The sign or "target" for pages apparently lacking from the document photographed is "Missing Page(s)". If it was possible to obtain the missing page(s) or section, they are spliced into the film along with adjacent pages. This may have necessitated cutting thru an image and duplicating adjacent pages to insure you complete continuity.
2. When an image on the film is obliterated with a large round black mark, it is an indication that the photographer suspected that the copy may have moved during exposure and thus cause a blurred image. You will find a good image of the page in the adjacent frame.
3. When a map, drawing or chart, etc., was part of the material being photographed the photographer followed a definite method in "sectioning" the material. It is customary to begin photoing at the upper left hand corner of a large sheet and to continue photoing from left to right in equal sections with a small overlap. If necessary, sectioning is continued again — beginning below the first row and continuing on until complete.
4. The majority of users indicate that the textual content is of greatest value, however, a somewhat higher quality reproduction could be made from "photographs" if essential to the understanding of the dissertation. Silver prints of "photographs" may be ordered at additional charge by writing the Order Department, giving the catalog number, title, author and specific pages you wish reproduced.
5. PLEASE NOTE: Some pages may have indistinct print. Filmed as received.

Xerox University Microfilms

300 North Zeeb Road
Ann Arbor, Michigan 48106

74-6993

YERG, Jr., Martin Charles, 1942-
AN OPTIMAL SAMPLING AND ANALYSIS METHODOLOGY.

The University of Oklahoma, Ph.D., 1973
Physics, meteorology

University Microfilms, A XEROX Company, Ann Arbor, Michigan

THE UNIVERSITY OF OKLAHOMA

GRADUATE COLLEGE

AN OPTIMAL SAMPLING AND ANALYSIS METHODOLOGY

A DISSERTATION

SUBMITTED TO THE GRADUATE FACULTY

in partial fulfillment of the requirements for the

degree of

DOCTOR OF PHILOSOPHY

BY

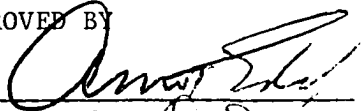
MARTIN CHARLES YERG, JR

Norman, Oklahoma

1973

AN OPTIMAL SAMPLING AND ANALYSIS METHODOLOGY

APPROVED BY

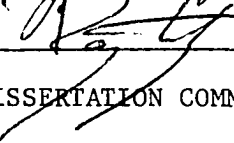


Michael D. Devine

John C. Bridges

David E. Duff

Eugene M. Williams



DISSERTATION COMMITTEE

ACKNOWLEDGEMENTS

For the past five years, Amos Eddy has been the motivating force behind my academic accomplishments. My present level of proficiency has been attained because he gave me the proper amounts of direction, freedom, encouragement and criticism at the right times. He is the one who taught me to regard all sciences (physical and social) as interdependent systems. I hope that my future work reflects some of his ability for problem solving and his genius of foresight.

Much of my work has relied on the encyclopedic knowledge of E. Pat Avara of the Atmospheric Sciences Laboratory at White Sands Missile Range, New Mexico. He has always been available for consultation with me. His ideas on the interplay of various mathematical techniques as well as on the formulation of the basic problem form the backbone to the optimal sampling and analysis methodology contained in this paper.

I have had the continual cooperation and interest of Drs. Claude Duchon, Eugene Wilkins, John Brixey, Ray Lutz and Michael Devine during the period of my research. Discussions with each of them have provided many improvements in my basic ideas.

I also recognize the help I received in various forms from Marvin Kays, Dr. E. R. Reinelt, Dr. Stig Rossby, King Sum Mok, Margaret Eddy and last, but not least, my wife, Ivy.

The funding of this research over the past three years has come from the National Science Foundation (NSF). The use of the computer facility at the National Center for Atmospheric Research (sponsored by NSF) has been invaluable to my work.

TABLE OF CONTENTS

Chapter		Page
I.	INRODUCTION.....	1
II.	THE OBJECTIVE ANALYSIS.....	4
III.	THE SIGNAL AND NOISE.....	10
IV.	THE OPTIMIZATION PROCEDURE....	20
V.	THE RESULTS.....	32
VI.	SUMMARY AND CONCLUSIONS.....	75
	LIST OF REFERENCES.....	80

AN OPTIMAL SAMPLING
AND
ANALYSIS METHODOLOGY

CHAPTER I

INTRODUCTION

Efficient sampling schemes for an experimental project or for routine observations may be found using different approaches to the placement of sensors in a space-time (x,y,z,t) volume. One approach might try to configure the sampling network based upon climatological considerations. Another might attempt to use a subset or an extension of available existing networks. Still another might rely upon the area of classical experimental design to dictate sampling concepts. Previous attempts to specify 'optimal' sampling networks for meteorological parameters have been reported by Gandin, et al., 1967; Baer and Withee, 1971; Northrup, et al., 1972; Kasahara, 1972; and Alaka and Elvander, 1972.

The methodology suggested here for selecting a sampling scheme uses the techniques of nonlinear optimization with stepwise regression, a generalized approach to objective analysis based upon multiple regression, and an exact definition of the goals of the sampling. In this paper, these ideas have been applied to a specific problem which

is how to sample a scalar phenomenon in a space-time volume using sensors on aircraft in order to produce an optimal signal analysis for a specified set of points when a number of constraints have been placed on the available resources and their use. This optimal sampling and analysis methodology, nevertheless, is generally applicable to many forms of experimentation and to most types of routine observational requirements. Besides the results presented here, the application of this methodology has been conceived for the problems of routinely observing the mesoscale wind field over irregular terrain and of providing the data input to numerical weather prediction models.

So far, simulation has provided the primary testing method for the sampling ideas. Simulation allows for the interpretation of the effects of various levels of complexity assumed for the problem through the existence of a known input signal. However, even though simulated data may be made to appear similar to real data, the test of a real field experiment with all the associated sensor failures, recording malfunctions, etc., still remains. Even so, simulation has the ability to present ideas on the importance of scale size, on the trade-off between several, relatively inaccurate sensors and a few, highly accurate ones, and on the feasibility of obtaining the desired results for a field exercise with the available resources. And, simulation can do all this without the expense and time required for field experimentation.

The deployment of a sampling system in a space-time volume can determine, by itself, the success or failure of any experimental effort.

However, many other considerations must enter into the total experimental process, such as instrumental calibration, noise analysis, data quality control, etc. The optimal methodology presented here deals only with the sampling and analysis aspects of the data handling problem with the other areas of the experimental process left for subsequent research.

CHAPTER II

THE OBJECTIVE ANALYSIS

The objective analysis technique used with the optimal sampling methodology is based upon multiple regression. Modifications have been made to the basic analysis procedure which make use of the structural characteristics of meteorological parameters and some of the types of noise usually associated with observing them. This objective analysis scheme has been presented in detail by Eddy, 1973 and applied to meteorological data by Lacy, 1973. Only a brief outline of the analysis procedure will be given here along with its connection with the sampling methodology.

Consider the model for the atmospheric signal which is to be sampled and analyzed as

$$Y = X \beta + \epsilon \quad \dots\dots\dots(1)$$

(NxJ) (NxM)(MxJ) (NxJ)

where $E(\epsilon) = 0$ and $COV(\epsilon_{ij}, \epsilon_{kj}) = V\sigma_{\epsilon}^2$ where V is a positive, definite matrix which contains the variance-covariance relationships of the noise, ϵ , and $COV(\epsilon_{ij}, \epsilon_{i\ell}) = 0$. Essentially, this model says that the elements of the Y matrix (consisting of N realizations of parameter values at J predictand locations) has some linear relationship (expressed by the β matrix) to the X matrix elements (consisting

of H realizations of parameter values at M predictor locations).

Upon minimizing the error sum of squares, an estimate of the coefficients may be obtained using the normal equations,

$$\hat{\beta} = (X^t V^{-1} X)^{-1} (X^t V^{-1} Y).$$

In general, if the elements of the $X^t V^{-1} X$ matrix were obtained from sampled data of sufficient resolution, the matrix would be nonsingular. Also, this matrix would be nonsingular, in general, for simulated data in that the model (equation 1) is usually an attempt to simplify the analytic representation of the signal. Thus, for each set of parameter values at the M predictor locations taken N times, ($N \geq M$), a set of M weights may be found whereby an estimate of the true value of the predictand matches the assumed signal in a least squares sense using

$$\hat{Y}_j = X \hat{\beta}_j$$

where \hat{Y}_j and $\hat{\beta}_j$ represent the estimates of the true signal and the set of M weights for the j th predictand.

For example, if one assumed that the temperature at Oklahoma City (OKC) were linearly related to the temperatures at Dallas-Fort Worth (FTW), Tulsa (TUL) and Dodge City (DDC), it might be expressed using equation 1 where $J=1$, $M=3$, $V=I$ and N could be 10. The predictand location (OKC) and the location of the predictors (FTW, TUL, DDC) would be given a relative definition in x, y, z, t . Then, after collecting 10 realizations of the temperatures at OKC, TUL, FTW, DDC for the particular time-space configuration defined, a $\hat{\beta}$ vector could be

obtained. At a future time, this $\hat{\beta}$ vector could be employed to provide an estimate of the temperature at OKC using the appropriate observations of temperature from FTW, TUL, DDC. However, the initial estimate of the true weights required N observations at the predictand point; a requirement which may not be easily attained.

The major modification to the basic regression scheme is to assume that the underlying relationships between the predictors and the predictands are known, or can be estimated. Thereby, the model for these variance-covariance relationships is given. Likewise, the variance-covariance relationships of the noise could be provided using a model for the noise such as a linear first-order Markov process. With these two matrices available, i.e., X^tY (or X^tX) and V , any vector, $\hat{\beta}_j$, can be completely determined using the following expression for the kth, l th element of a quadratic form,

$$A^tB^{-1}A)_{k,l} = \sum_{i=1}^N \sum_{j=1}^N a_{ik}a_{jl}b_{ij}^{-1} \dots\dots\dots(2)$$

where a_{ij} is the i th, j th element of A and similarly for b_{ij}^{-1} and B^{-1} . This modification does not require the vector of observations at the predictand locations as was required previously.

Another modification is necessary, however, because the basic multiple regression model assumes the observations at the M sample points contain only signal and no error. Yet, real experimental observations not only contain signal, but they also contain inseparable amounts of noise. In fact,

$$X = X_s + \alpha$$

where X_s is the signal portion of the observation and α is the noise portion which may reasonably be defined similarly to ϵ , i.e.,

$$E(\alpha) = 0 \text{ and } \text{COV}(\alpha_{ij}, \alpha_{kj}) = V\sigma_\alpha^2 \text{ and } \text{COV}(\alpha_{ij}, \alpha_{i\ell}) = 0.$$

Using this knowledge, a new set of weights must be derived in order that the estimate of the signal at a predictand location match the assumed signal in a least squares sense. The new weights, $\tilde{\beta}_j$, become

$$\tilde{\beta}_j = (X_s^t X_s + \alpha^t \alpha)^{-1} X_s^t X_s \hat{\beta}_j . \quad \dots\dots\dots(3)$$

The use of these weights with the appropriate set of observations will give the desired signal analysis at a predictand location as follows

$$\tilde{Y}_j = X \tilde{\beta}_j .$$

Essentially, the optimal sampling algorithm will attempt to pick the particular set of observation locations in space and time which will give a desired definition to the signal for a specified set of predictand locations. The multiple correlation coefficient is a measure of the amount of variance in the predictand which is explained by a particular set of predictors. Thus, this parameter will be used as the link between the analysis and the optimal sensor deployment.

Let us define the multiple correlation coefficient for the single predictand vector, Y_j , as

$$R_j = \frac{\text{COV}(Y_j, \tilde{Y}_j)}{\{\text{VAR}(Y) \text{ VAR}(\tilde{Y})\}^{1/2}}$$

or,

$$R_j = \frac{Y_j^t V^{-1} \hat{Y}_j}{(Y_j^t V^{-1} Y_j)^{1/2} (\hat{Y}_j^t V^{-1} \hat{Y}_j)^{1/2}}$$

It can be shown that

$$R_j^2 = \frac{Y_j^t V^{-1} \hat{Y}_j}{Y_j^t V^{-1} Y_j} \dots\dots\dots(4)$$

where $0 < R^2 \leq 1$. The amount of variance unexplained may be expressed as $1 - R_j^2$ for any jth predictand location. Therefore, the particular set of observation locations to select for obtaining an optimal signal analysis would be that set of locations which minimized the amount of unexplained variance at each of the J predictand locations.

The problem becomes how to select the predictor locations in order to find

$$\text{MIN} \left\{ \sum_{j=1}^J (1 - R_j^2) \right\}$$

for every possible observational configuration.

Because the space-time volume has been defined for x, y, z, t , the set of M predictor locations (whose N observational values have been represented by the matrix X) must be defined for each of the four coordinates. Thus, the actual solution vector (where to place the sensors in order to collect observations) to the minimization problem will have dimensions $4 \cdot (M \times 1)$. Likewise, each of the J predictand locations (whose N observational values have been represented by the vector Y_j) must be specified as to their location in the

space-time volume.

It should be noted that when deriving the variance-covariance relationships between the signal (or the noise) at points in the space-time volume, the assumption is that each matrix operation has been done with an infinite amount of data, i.e., the matrix operations were done in an expected value sense. Thus, the $X^t X$ term becomes $X_S^t X_S + \alpha^t \alpha$ because the signal and noise are assumed independent and for an infinite amount of data, $X_S^t \alpha$ would be zero.

CHAPTER III

THE SIGNAL AND NOISE

Both the objective analysis technique and the optimization scheme require only that some structural definition be given to the phenomenon to be observed and the noise associated with the observing it. The definitions may be analytical or empirical. Once the sampling and analysis locations have been determined, the experimental process or routine observational method will provide the actual observations needed for the objective analysis. However, when the entire process is being done using simulation, both the variance-covariance relationships and the actual signal and noise definitions must be available.

For the work of this paper, an analytic expression has been used to describe the atmospheric signal continuously over a time-space volume. The expression is meant to be illustrative. In order to provide the variance-covariance relationships required by the optimal sampling methodology, certain parameters of the expression have been given analytic and empirical distributions based upon research work conducted by Reinelt, 1973.

The signal has been expressed as

$$s_i = A e^{-\alpha_1 (\omega_1 x'_i)^2 - \alpha_2 (\omega_2 y'_i)^2 - \alpha_3 t_i'^2} \cos(\omega_1 x'_i) \cos(\omega_2 y'_i) \cos(\omega_3 z'_i + \phi) \dots \dots \dots (5)$$

where s_i is the value of the function at the point defined by x_i , y_i , z_i , t_i and

$$\begin{aligned}x_i' &= x_i - (x_0 + c_x t_i'), \\y_i' &= y_i - (y_0 + c_y t_i'), \\ \text{and } t_i' &= t_i - t_0.\end{aligned}$$

The amplitude of the system is A ; α_1 , α_2 , α_3 are the dampening factors in the x , y , t directions respectively; ω_1 , ω_2 , ω_3 represent the frequency in the x, y, z directions respectively; and ϕ is the phase shift in the vertical. The system origin is at x_0, y_0, t_0 and $z_0=0$. Its propagation speed is c_x and c_y in the x and y directions respectively. The parameters A , ω_1 , ω_2 and ϕ have been given independent Gaussian distributions as follows

$$\begin{aligned}A &\sim N(a, \sigma_a^2) \quad , \\ \omega_1 &\sim N(\mu_1, \sigma_1^2) \quad , \\ \omega_2 &\sim N(\mu_2, \sigma_2^2) \quad , \\ \text{and } \phi &\sim N(\mu_3, \sigma_3^2) \quad .\end{aligned}$$

The parameters x_0 , y_0 , t_0 , c_x and c_y may be given empirical distributions during the optimization process as will be shown.

Figure 1 (a,b,c) provides a visual illustration of this signal function for a particular set of input parameters. At each time step, the value of the function has been contoured on an x, y grid for three levels in z .

The parameters of the expression for the atmospheric signal which have analytic distributions have been intergrated out in the

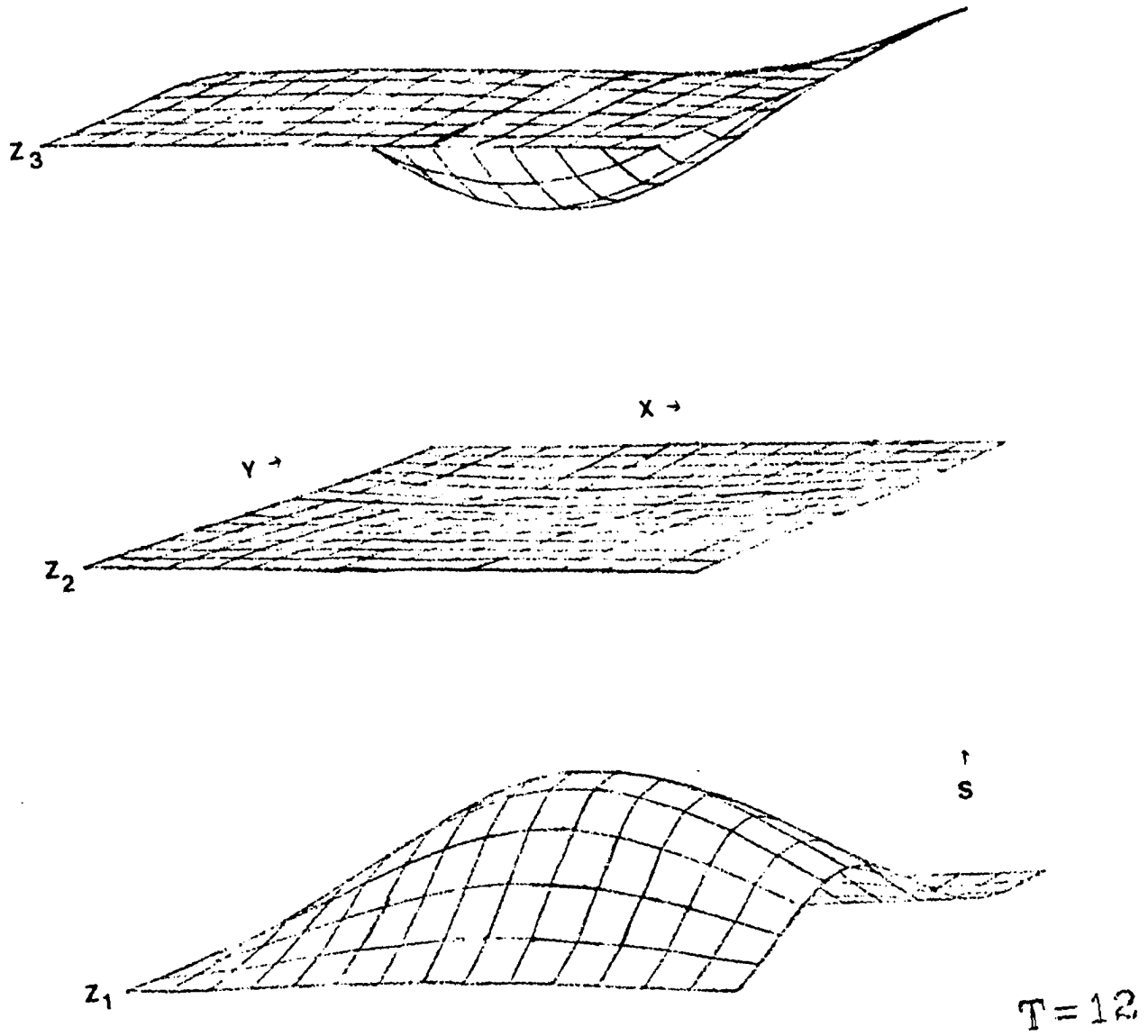


Figure 1b: A three-dimensional look at the signal function, equation (5), for $t_0 = 10$.

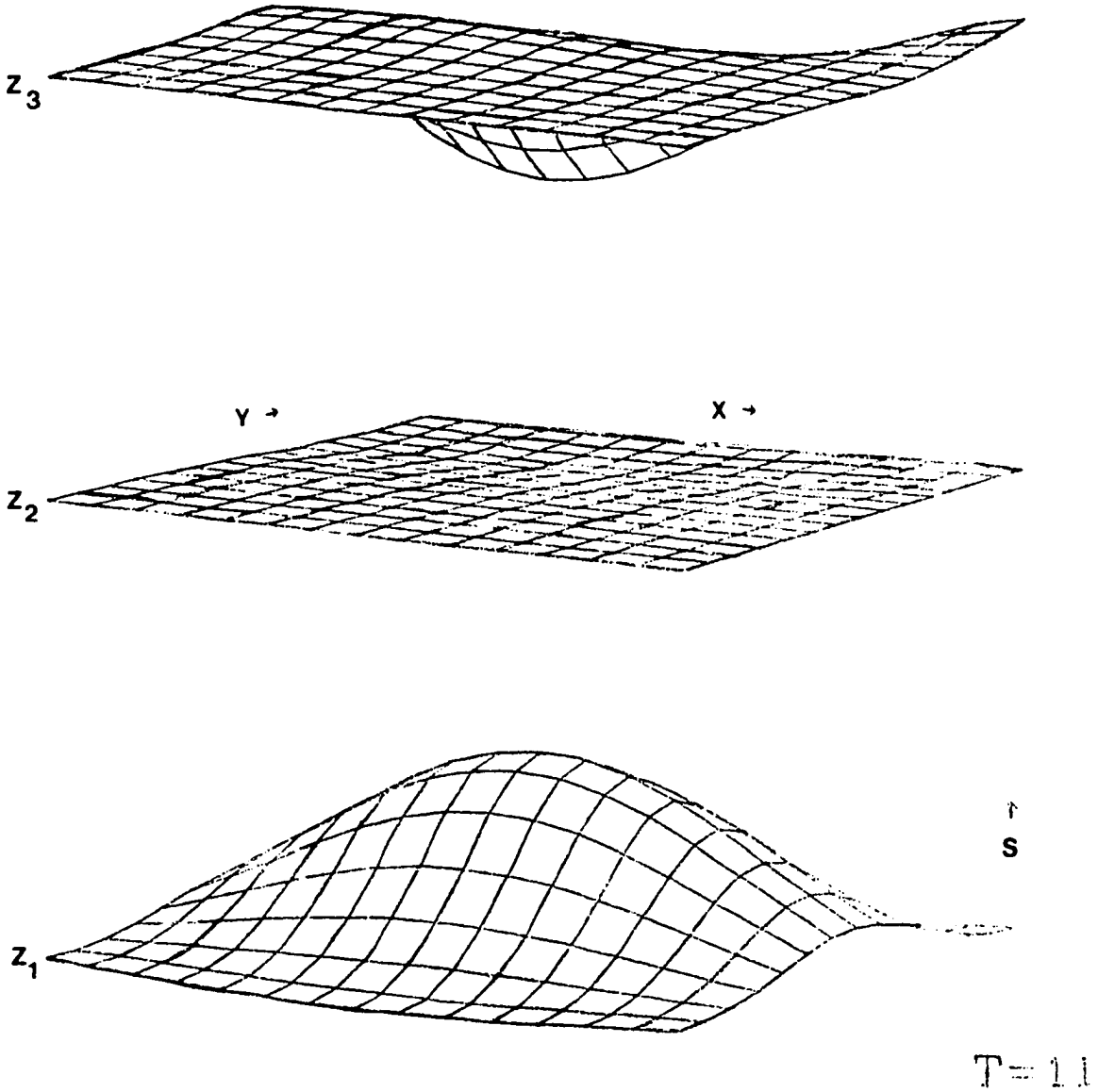


Figure 1a: A three-dimensional look at the signal function, equation (5), for $t_0 = 10$.

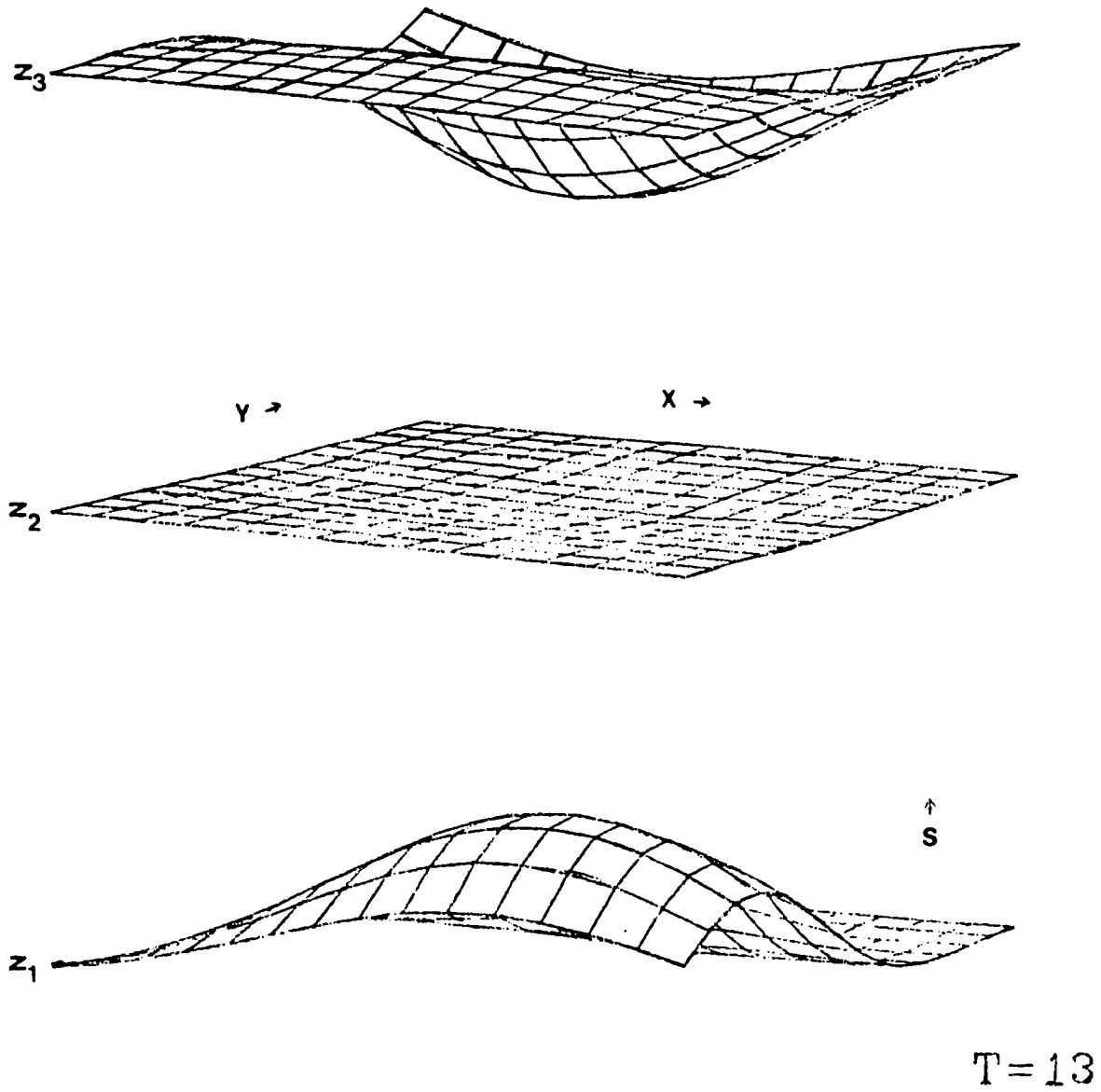


Figure 1c: A three-dimensional look at the signal function, equation (5), for $t_0 = 10$.

usual manner to obtain both the first moment and the second moment about the mean. The latter expression is used for the variance-covariance relationships required by the optimization process.

The results are that the expected value of the signal is

$$E(s_i) = E(A) e^{-\alpha_3 t_i'^2} E\{ e^{-\alpha_1 (\omega_1 x_i')^2} \cos(\omega_1 x_i') \} \\ E\{ e^{-\alpha_2 (\omega_2 y_i')^2} \cos(\omega_2 y_i') \} E\{ \cos(\omega_3 z_i + \phi) \}$$

which becomes

$$E(s_i) = a e^{-\alpha_3 t_i'^2} (P_i Q_i)^{-1/2} \cos\left(\frac{\mu_1 x_i'}{P_i}\right) \cos\left(\frac{\mu_2 y_i'}{Q_i}\right) \\ e^{-\left[\frac{\sigma_1^2 x_i'^2 - \eta_1}{2P_i} + \frac{\sigma_2^2 y_i'^2 - \eta_2}{2Q_i} + \frac{\eta_1 + \eta_2 + \sigma_3^2}{2} \right]} \\ \cos(\mu_3 + \omega_3 z_i) \dots\dots\dots (6)$$

where

$$P_i = 1 + 2\sigma_1^2 \alpha_1 x_i'^2, \\ Q_i = 1 + 2\sigma_2^2 \alpha_2 y_i'^2, \\ \eta_1 = (\mu_1 / \sigma_1)^2, \\ \text{and } \eta_2 = (\mu_2 / \sigma_2)^2.$$

And, the expression for the variance-covariances between point (x_i, y_i, z_i, t_i) and point (x_j, y_j, z_j, t_j) is

$$\begin{aligned}
 E(s_i s_j) &= E(A^2) E\{ e^{-\alpha_1 \omega_1^2 (x_i'^2 + x_j'^2)} \cos(\omega_1 x_i') \cos(\omega_1 x_j') \} \\
 &\quad E\{ e^{-\alpha_2 \omega_2^2 (y_i'^2 + y_j'^2)} \cos(\omega_2 y_i') \cos(\omega_2 y_j') \} \\
 &\quad E\{ \cos(\omega_3 z_i + \phi) \cos(\omega_3 z_j + \phi) \} e^{-\alpha_3 (t_i'^2 + t_j'^2)} \\
 &= (\sigma_a^2 + a^2) / 4 (P_{ij} Q_{ij})^{-\frac{1}{2}} e^{-\frac{1}{2} \alpha_3 (t_i'^2 + t_j'^2)} e^{\frac{1}{2} (\eta_1 + \eta_2)} \\
 &\quad \left[e^{\eta_3 \cos\left[\frac{\mu_1 (x_i' - x_j')}{P_{ij}}\right]} + e^{-\eta_3 \cos\left[\frac{\mu_1 (x_i' + x_j')}{P_{ij}}\right]} \right] e^{-\left[\frac{\sigma_1^2 (x_i'^2 + x_j'^2) - \eta_1}{2P_{ij}}\right]} \\
 &\quad \left[e^{\eta_4 \cos\left[\frac{\mu_2 (y_i' - y_j')}{Q_{ij}}\right]} + e^{-\eta_4 \cos\left[\frac{\mu_2 (y_i' + y_j')}{Q_{ij}}\right]} \right] e^{-\left[\frac{\sigma_2^2 (y_i'^2 + y_j'^2) - \eta_2}{2Q_{ij}}\right]} \\
 &\quad \left[\frac{1}{2} \cos(\mu_3 + \omega_3 z_i) \cos(\mu_3 + \omega_3 z_j) (1 + e^{-2\sigma_3^2}) \right. \\
 &\quad \left. + \frac{1}{2} \sin(\mu_3 + \omega_3 z_i) \sin(\mu_3 + \omega_3 z_j) (1 - e^{-2\sigma_3^2}) \right] \\
 &\quad \dots\dots\dots (7)
 \end{aligned}$$

$$\begin{aligned}
 \text{where } P_{ij} &= P_i + P_j - 1, \\
 Q_{ij} &= Q_i + Q_j - 1, \\
 \eta_3 &= \frac{\sigma_1^2 x_i' x_j'}{P_{ij}}, \\
 \eta_4 &= \frac{\sigma_2^2 y_i' y_j'}{Q_{ij}},
 \end{aligned}$$

and all other parameters are defined as before.

The distributions given A , ω_1 , ω_2 and ϕ are defined by the mean value and the variance of the parameter. Because of this, the expected value of the signal function along with the variance-covariance relationships just presented may be easily determined using climatological information about the parameters of the phenomenon being sampled. The definition given to the expected value and covariances of the signal function is still valid for any a posteriori estimate of the parameters' mean and variance if the a priori and a posteriori distribution functions are similar. Where this is not the case, either a reintegration is necessary using the new analytic distribution function or the new distribution of the particular parameter must be handled using empirical means.

For illustration, let us assume, as before, the a priori distribution of the parameter A is Gaussian with mean, a , and variance, σ_a^2 . If the a posteriori distribution of A can be assumed to remain Gaussian upon updating the estimates of the mean and variance of A (using mathematical techniques such as empirical orthogonal functions or linear discriminate analysis), the new mean, \hat{a} , and variance, $\hat{\sigma}_a^2$, would simply replace the former values in

equations (6) and (7). However, if the a posteriori distribution of A were still independent of the other parameters, but not Gaussian having instead a non-analytic shape, new expressions for $E(s_i)$ and $COV(s_i, s_j)$ would be necessary which do not include $E(A)$ and $E(A^2)$ as before. By dividing the new, non-analytic distribution for A into G sections, each with probability w_g and average value, a_g , the a posteriori expression for $E(s_i)$ could be estimated by

$$E(s_i) = \sum_{g=1}^G w_g a_g \hat{E}(s_i)$$

where $\hat{E}(s_i)$ is the new expression for $E(s_i)$ which does not include $E(A)$. The a posteriori expression of $COV(s_i, s_j)$ is similarly attained. This method of including non-analytic or empirical distributions is applicable to all of the parameters defining the signal function.

The noise portion of the observational data set used for the objective analysis is manifest in the minimization problem (equation (4)) as $\alpha^t \alpha = V \sigma_\alpha^2$. The selected model for the noise present on the true signal is a linear, first-order Markov process:

$$\alpha_i = \rho_1 \alpha_{i-1} + \gamma_i$$

where ρ_1 is the lag-one autocorrelation coefficient defined over the distance (space and/or time) between α_i and α_{i-1} and γ is Gaussianly distributed with $E(\gamma) = 0$ and $E(\gamma^2) = \sigma_\gamma^2$. This model allows for the noise values to be independent or correlated depending upon the value of ρ_1 . And,

$$E(\alpha_i) = 0$$

$$\text{COV}(\alpha_i, \alpha_j) = \rho_1^{|i-j|} \sigma_\alpha^2$$

where $\sigma_\alpha^2 = \frac{\sigma_Y^2}{1 - \rho_1^2}$ and $|i-j|$ represents the space-time distance between noise values at locations i and j .

If the signal-to-noise ratio (S/N) is defined as the average variance of the signal over all predictand locations in the space-time volume divided by the variance of the noise, i.e.,

$$S/N = \frac{\frac{1}{J} \sum_{j=1}^J E(Y^t Y)}{\text{VAR}(\alpha)} \quad \dots \dots \dots (8)$$

then, for any optimal sampling problem, a signal-to-noise ratio may be specified in order to note the influence of noise on the sampling and analysis results.

CHAPTER IV

THE OPTIMIZATION PROCEDURE

Because of the form of the minimization problem (equation (4)), the optimization procedure employed is a nonlinear programming (NLP) algorithm. The basic NLP problem may be stated as

$$\begin{aligned} & \text{minimize } f(Z) \quad , \quad Z \in E^n \\ & \text{subject to } h_i(Z) = 0 \quad , \quad i=1,2, \dots, m \\ & \quad \quad \quad g_i(Z) \geq 0 \quad , \quad i=m+1, \dots, p \end{aligned}$$

where Z is a vector which is defined in n -dimensional Euclidean space, $f(Z)$ represents the objective function to be optimized, $h_i(Z)$ represents the m equality constraints while $g_i(Z)$ handles the $p-m$ inequality constraints and all the functions may be nonlinear. The optimal solution vector, Z^* , is defined as the vector which satisfies the conditions of the problem.

For our case, $f(Z) = \sum_{j=1}^J (1-R_j^2)$ where the decision variables

essentially are

$$Z^t = (x_1, y_1, z_1, t_1, \dots, x_M, y_M, z_M, t_M)$$

which is a vector of M sample point coordinates in 4-space where M observations will be taken in order to provide the values of X .

Because the sensors are attached to aircraft, the equality and inequality constraint set will restrict the M locations in the space-time volume at which the sensors may be placed in a manner consistent with aircraft flight capabilities. The set of M predictor locations in 4-space which give a minimum value to $f(Z)$ and which will also satisfy the constraint set will be an optimal solution vector, Z^* .

The NLP algorithm which has been chosen to find the optimal solution to the sampling problem is the Flexible Tolerance method of Paviani and Himmelblau (1969). The Flexible Tolerance method is basically a direct search procedure. This class of optimization algorithms does not use analytic approaches such as gradients or second derivatives to find an optimal solution, but instead relies on determining each new decision variable vector from successive evaluations of the objective function only. These successive evaluations determine the direction and the speed of movement of the search process in W -space where W is the number of independent decision variables.

The Flexible Tolerance algorithm uses both the flexible polyhedron search of Nelder and Mead (1964) and a procedure for checking the degree by which each potential solution vector violates the constraint set. The Nelder and Mead search method operates on the idea of rejecting the highest value of the objective function evaluated at $W+1$ vertices of a polyhedron and reflecting that vertex through the centroid of the remaining vertices. The polyhedron may expand or contract as it searches for the optimum. In the limit, all $W+1$

vertices will contract to a single solution point. The degree by which each potential solution vector disobeys the constraint set also contracts during the search process until the constraint set holds exactly at the optimal point. In actual practice, the Flexible Tolerance method collapses to within an ϵ tolerance of the optimum and the constraint set is met within a corresponding tolerance.

The objective function which will yield a statistically best objective analysis over a set of J predictands has been expressed as:

$$f(Z) = \sum_{j=1}^J (1-R_j^2)$$

where

$$1-R_j^2 = 1 - \frac{Y_j^t X (X^t X + \alpha^t \alpha)^{-1} X^t Y_j}{Y_j^t Y_j}$$

and the Z vector contains the locations of the M sample points, and the effect of the noise on the model of the atmospheric signal (equation (1)) cancels.

Because of the use of R_j^2 , the objective function, as stated, only represents the percentage variance. The following modification is made in order to minimize the actual variance

$$f(Z) = \sum_{j=1}^J \delta_j \{ Y_j^t Y_j - Y_j^t X (X^t X + \alpha^t \alpha)^{-1} X^t Y_j \}.$$

Since the possibility exists that the reduction of actual variance at some of the J points is more important than at other points, a set of weights, δ_j , allow the consumer to express analytically the usefulness of reduced variance at individual points in the

objective analysis space. This corresponds to a multiple-dimensional, discrete utility function. Thus, defining a very accurate point value of a meteorological parameter might be more useful near a population center than elsewhere even though the variance in the analyzed value would ordinarily be quite small there.

Noting that a modelled covariance function will be employed to obtain the components of each of the J elements in the objective function, we could include the effect of empirical distributions for P independent parameters to these modelled covariances by using weights, ψ_ℓ , over the L_p divisions in the p th empirical function. The final form of the objective function thus becomes

$$f(Z) = \sum_{p=1}^P \sum_{\ell=1}^{L_p} \psi_\ell \sum_{j=1}^J \delta_j \{Y_j^t Y_j - Y_j^t X_S (X_S^t X_S + \alpha^t \alpha)^{-1} X_S^t Y_j\} \dots (9)$$

This objective function can be minimized by finding the locations in time and space at which to place sensors in order to sample the signal function.

The constraint set has been formulated from considerations of the requirements of the optimization process and the restrictions on aircraft sampling movements. The former considerations essentially desire decision variables which have similar scale sizes and effect on the optimization process. The latter includes the requirement that aircraft take off and

land at only specific locations without running out of fuel, and, for our case, that the aircraft fly in straight lines while sampling. Even though the straight-line flight requirement will necessitate a change in the decision variable vector used with the search technique, this restriction on the aircraft movements provides a degree of simplicity to field operations, and eliminates some of the corrections which must be made to the data sets collected during the period in which the aircraft is accelerating and turning.

Because of the nature of the problem being considered, no explicit resource allocation constraints have been included. In general, research aircraft are already equipped with sensing devices and the problem is how to utilize these sensors in an optimal fashion to produce the desired results. However, the problem of whether to use a few expensive, highly accurate instruments or many inexpensive yet relatively inaccurate ones could also be a part of the overall optimizing process. The solution could be obtained by comparing the cost of using certain numbers of each sensors type versus the utility of the degree of accuracy in the analyzed signal. (Note that even the most precise instrument system might not be capable of yielding a minimum acceptable accuracy in the analyzed signal.)

The larger problem of how to allot the available resources for a multipurpose experiment conducted over an extended period requires more investigation than is presented in this paper.

The constraint set is formulated as follows:

Let N represent the maximum number of sensor locations considered for the experiment and N_q represent the number of possible sensors placed on the q th leg of the aircraft path, $q = 1, 2, \dots, Q$. (Q is the maximum number of possible straight line paths considered reasonable for this experiment.) Then,

$$\sum_{q=1}^Q N_q \leq N .$$

(Note that any N_q could be zero.) Also, let the flight path be restricted so that the aircraft travels a nearly closed path where each sensor could be placed a γ distance apart for each leg.

$$\sum_{q=1}^Q \gamma N_q \sin \theta_q \leq \delta$$

$$\sum_{q=1}^Q \gamma N_q \cos \theta_q \leq \delta$$

where θ_q is the angle between each leg of the flight path and the positive x direction. The level of the aircraft for each leg is considered constant and represented by z_q . Thus, the new decision variables to be used by the search process are N_q , θ_q , and z_q .

Having selected all the possible leg orientations and lengths as well as heights, all the possible places to put sensors can be derived using

$$\begin{aligned}\Delta x_q &= \gamma \cos \theta_q , \\ \Delta y_q &= \gamma \sin \theta_q , \\ \text{and } \Delta t_q &= \delta_t\end{aligned}$$

where Δx_q and Δy_q are the x, y distances between possible sensor locations on the qth leg and the time distance between the possible sample points is a constant δ_t for the entire flight. Then,

$$\begin{aligned}\hat{x}_i &= {}^q x_o + i \Delta x_q , \\ \hat{y}_i &= {}^q y_o + i \Delta y_q , \\ \hat{z}_i &= z_q , \\ \text{and } \hat{t}_i &= {}^q t_o + i \delta_t\end{aligned}$$

for $i = 1, 2, \dots, N_q$ and $q = 1, 2, \dots, Q$. The ${}^q x_o$, ${}^q y_o$ and ${}^q t_o$ represent the origin of the qth leg, where at least one origin must be specified. The circumflexes indicate that the coordinates are those selected by the optimization process as possible sample points.

All of the sensor locations calculated above satisfy the straight-line flying requirements, but they do not necessarily satisfy the constraints restricting the total number of sensors allowed. If there were resource allocation constraints, the cost versus utility of each of the sensor locations must also be evaluated. Both of these considerations may be handled using a suboptimization scheme based upon stepwise regression after Efron (1962).

This process will be illustrated for a single predictand with the necessary extension explained later. Form the matrix of covariance

between all the possible predictors and the predictand:

$$F_j = \begin{bmatrix} X_s^t X_s + \alpha^t \alpha & X_s^t Y_j \\ Y_j^t X_s & Y_j^t Y_j \end{bmatrix} = \begin{bmatrix} r_{1,1} & r_{1,2} & \cdots & r_{1,M} & r_{1,M+1} \\ r_{2,1} & r_{2,2} & \cdots & r_{2,M} & r_{2,M+1} \\ & & \cdot & & \\ & & & \cdot & \\ r_{M+1,1} & \cdots & & & r_{M+1,M+1} \end{bmatrix}$$

Having been given the coordinates of each of the possible sample points, all of the elements in the F_j matrix are available. For the initial matrix, ${}^{(0)}r_{k\ell} = \text{COV}(s_k, s_\ell)$ where the superscripts indicate the stage of the stepwise regression process.

Now, test the parameters, \tilde{R}_i ,

$${}^{(0)}\tilde{R}_i = \frac{{}^{(0)}r_{i,M+1} \quad {}^{(0)}r_{M+1,i}}{{}^{(0)}r_{i,i}}$$

for $i = 1, 2, \dots, M$, and select the largest, say the k th, element. The ratio will indicate the sensor which explains the most variance present in the predictand of all possible sensors because it is most correlated with that predictand. After pivoting on the k th, k th element, the process is repeated. The stopping criteria employed for this stepwise regression process include (1) stop when the number of allowable sampling points has been met, (2) stop when the percentage variance explained by any additional sensor is below .1% and (3) stop when the variance explained in the predictand point exceeds 99%.

The method chosen to handle all the predictands considered for the objective analysis is to form this matrix:

$${}^{(0)}F' = \begin{bmatrix} X_s^t X_s + \alpha^t \alpha & X_s^t Y \\ Y^t X_s & Y^t Y \end{bmatrix}$$

where the dimensions of Y have been expanded to include all the predictand points. The test for reduction in variance would be over all the predictands as follows

$${}^{(g)}\tilde{R}_i = \sum_{j=1}^J {}^{(g)}\tilde{R}_{ij} = \frac{\sum_{j=1}^J {}^{(g)}r_{i,M+j} {}^{(g)}r_{M+j,i}}{({}^{(g)}r_{i,i})}$$

The largest ${}^{(g)}\tilde{R}_i$ would then be used to decide the elements to enter the regression and the pivot would be carried out on the entire ${}^{(g)}F'$ matrix. After the subset of all possible sampling locations has been selected by the stepwise regression technique, they are used in the previously defined Z vector to evaluate the objective function.

Other constraints enter into the optimization process. Among these is one which requires the aircraft to land before the fuel supply is depleted:

$$\sum_{q=1}^Q N_q \delta_t \leq U_t$$

where U_t is an upper limit on the possible aircraft flight time. And, another set of constraints are used to help the optimization algorithm converge faster by keeping all N_q positive or zero:

$$N_q \geq 0 \quad \text{for } q = 1, 2, \dots, Q.$$

For the use by the optimization procedure, all decision variables (N_q, θ_q, z_q) are scaled to the same order of magnitude.

Many other constraints are possible for the optimization problem, but are not a part of the constraint set used for this report. For instance, the cost of sampling at each point or for the entire exercise may be restricted by a specific amount. This constraint might better show the trade-off between few, expensive, but accurate sensors versus many, inexpensive yet relatively inaccurate ones.

As implemented using the direct search to optimization, this methodology may have many applications and can handle many different kinds of constraints. The suboptimization could be eliminated in order that all possible sensor locations be considered. At present, the decision variables (N_q, θ_q, z_q) are not required to be integer. However, any number of these variables could be made integer during the optimization process simply by having the direct search process only consider integer values where desired. Realizing the variations possible in the optimal sampling problem, the NLP optimization approach of direct search is highly recommended because of its "hands on" capabilities.

Figure 2 shows a schematic diagram of the optimization algorithm as used for this research. The basic search method follows the Flexible Tolerance procedure with the addition of a suboptimization problem.

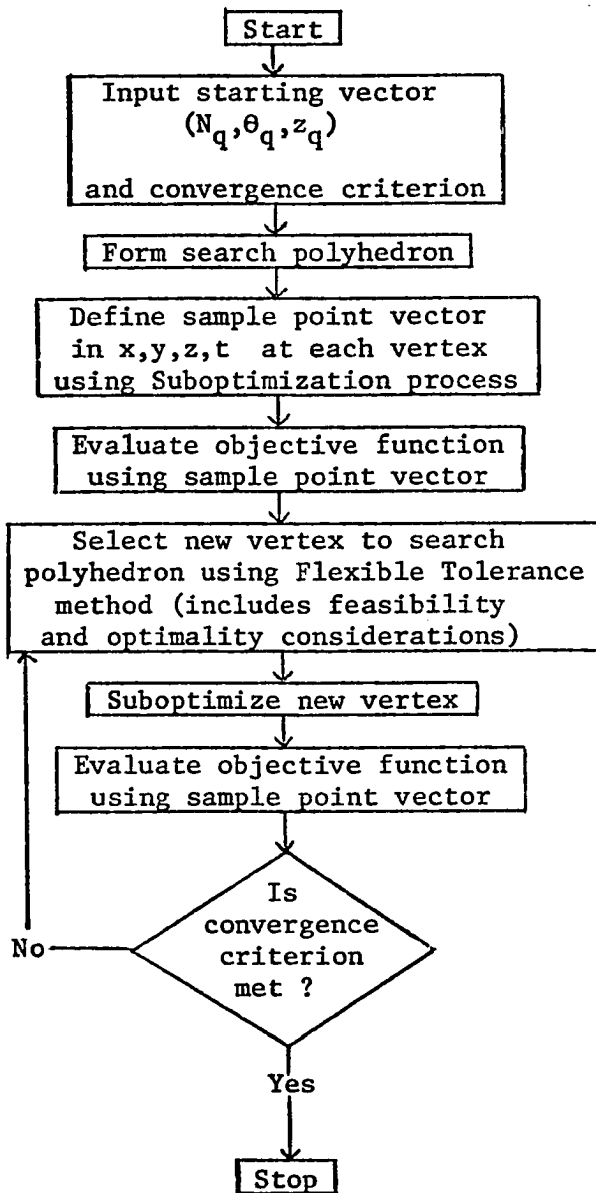
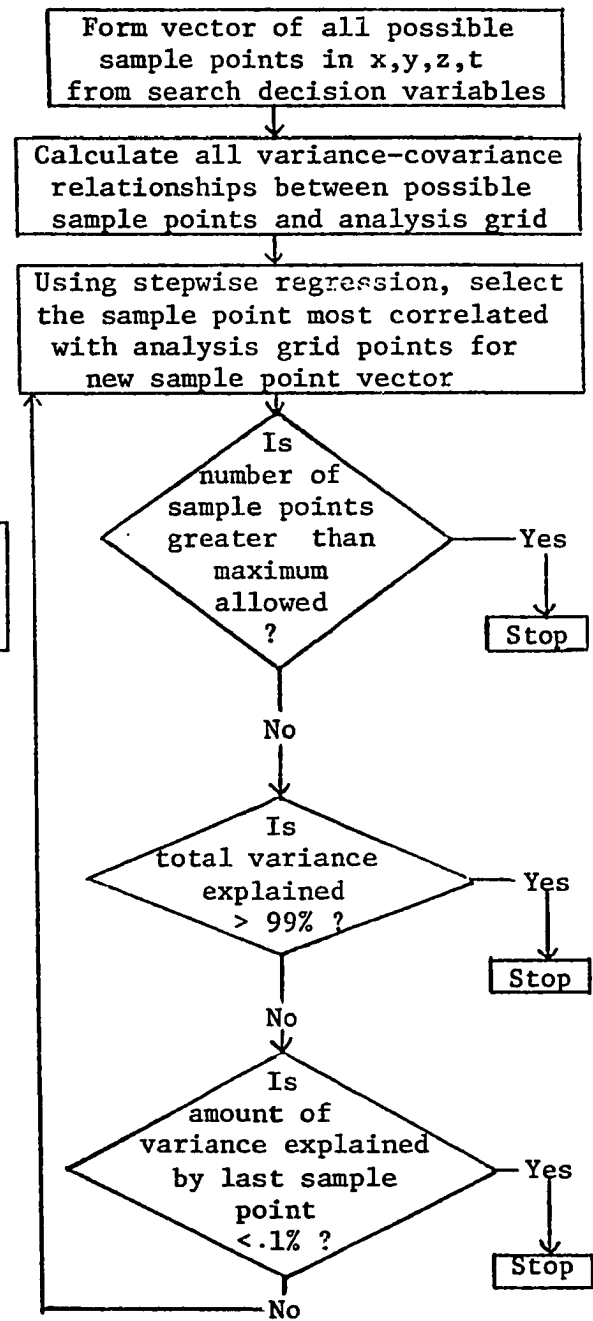
BASIC SEARCH ALGORITHMSUBOPTIMIZATION PROCESS

Figure 2: A schematic diagram showing the optimization procedure used in the optimal sampling and analysis methodology.

For the NLP purist, one feature of the methodology might be bothersome. The particular objective function used is highly complex and many local optima exist, i.e., many Z vectors may represent the smallest value of $f(Z)$ within their immediate vicinity. (The minimum of all local minima is the global minimum.) Thus, for any starting vector, the solution vector and value of the objective function found by the optimization process will not necessarily be the same as found with another starting vector. Usually, in such a case, the optimization process is repeated a number of times with different input vectors and the most optimal of all the solutions declared the global optimum. Different input vectors may be supplied for this problem by selecting various geometric patterns for the proposed aircraft flight plan. As an extreme, a random number generator could even be used to provide the individual elements of the starting vector. However, as will be shown, the expense of resolving the NLP problem several times for different starting vectors may not be justified for the problem being considered, depending on the signal-to-noise ratio assumed.

Therefore, each solution vector for the problem of how to fly aircraft in a space-time volume in order to get an optimal signal analysis should be considered as only a locally optimum flight path and not as an absolutely unique or globally optimum solution.

CHAPTER V

THE RESULTS

For visual display and because of numerical weather prediction requirements, the predictand locations used for testing the optimal sampling and analysis methodology are regularly spaced. The regularly spaced grid selected consists of 49 points and might be thought of as corresponding to a portions of the NMC Octogonal Grid (figure 3). For instance, if the signal function was a representation of the Arctic High, the grid might be the subset of the NMC grid bordered by the points (17,11), (23,11), (23,17) and (17,17). Or, if the signal function attempted to represent divergence-convergence patterns of these Highs, the grid might fall within the NMC grid points of (18,12), (21,12), (21,15) and (18,15). The reference to the NMC grid and the particular areas mentioned is a result of the Arctic High pressure system investigation conducted by Reinelt, 1973 and the fact that historical data is readily available at NCAR for these grid locations.

Because of the grid location and orientation as suggested above, a basic set of parameter values has been chosen with which many of the tests on the optimal sampling and analysis methodology have been

NMC OCTAGONAL GRID

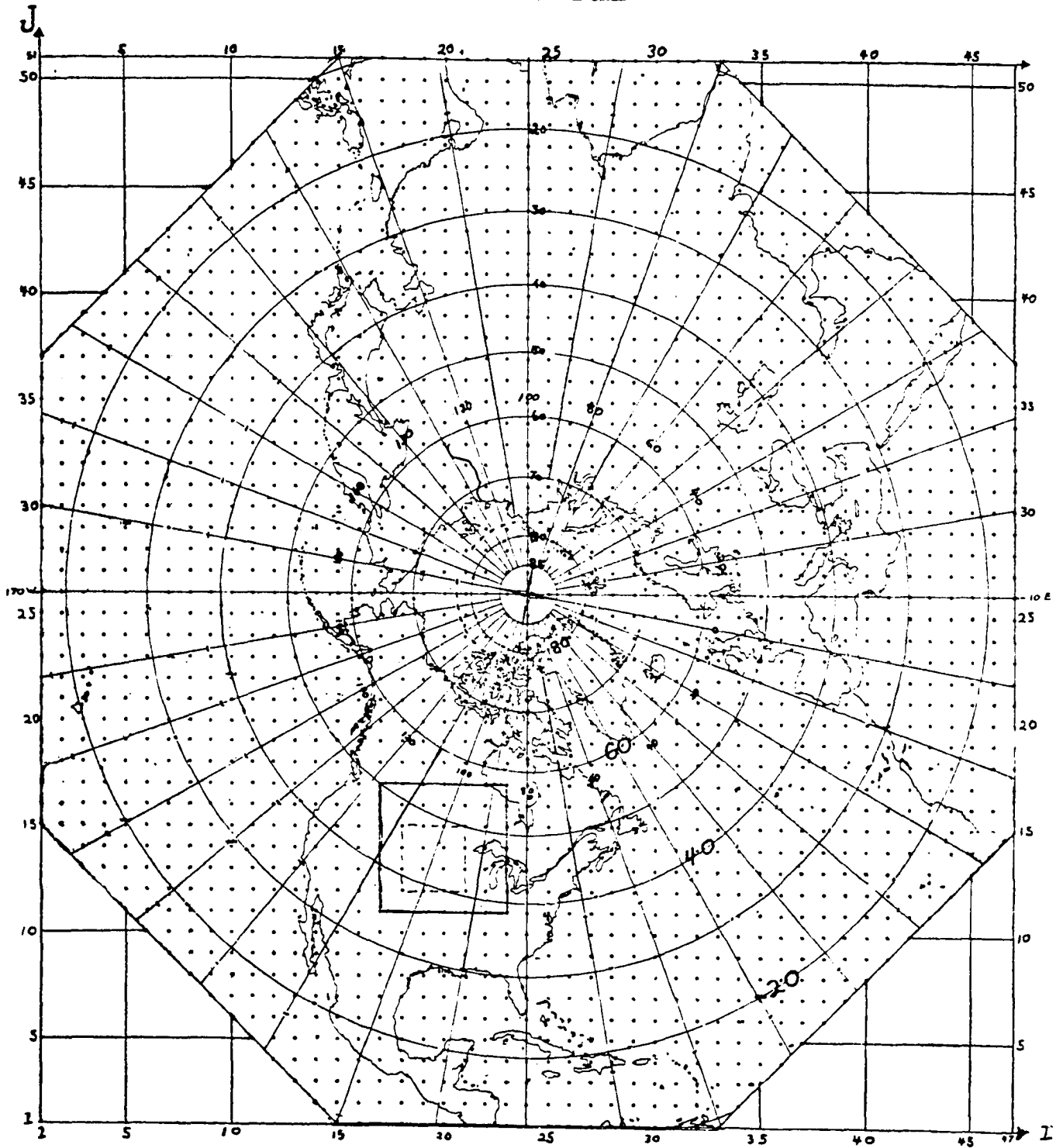


Figure 3. NMC 47x51 grid.
 There are 1977 data points in the octagon.
 The pole point is $I, J = 24, 26$.

run. They are

$$\text{for } A: \quad a = 5 \quad \text{and} \quad \sigma_a = .5$$

$$\text{for } \omega_1: \quad \mu_1 = 1 \quad \text{and} \quad \sigma_1 = .5$$

$$\text{for } \omega_2: \quad \mu_2 = .8 \quad \text{and} \quad \sigma_2 = .3$$

$$\text{for } \phi: \quad \mu_3 = 0^0 \quad \text{and} \quad \sigma_3 = 10^0$$

and

$$x_0 = 4. \quad \alpha_1 = .5 \quad c_x = .75$$

$$y_0 = 4. \quad , \quad \alpha_2 = .5 \quad , \quad c_y = -1.5 \quad .$$

$$t_0 = 2. \quad \alpha_3 = .1 \quad \omega_3 = .78$$

The shape and movement of this system for all $z_i = 0$ is shown in figures 4 through 6 as calculated by the expected value of the atmospheric signal (equation (6)). The true value of the analysis for a set of 49 grid points at $t = 2$ is shown in figure 7. This is the signal which will serve for all root-mean-square values calculated. Modifications to this basic signal will be specified as necessary.

The first set of tests run on the sampling algorithm was how to place sensors within the grid array in order that the sensors would be optimally placed for all time. For these tests, time was integrated out of each of the variance-covariance relationships using Gaussian Quadrature. Because of the nature of this problem, no objective analysis accompanies the optimal solution vector. The amount of unexplained variance at the grid locations for all time is, in general, quite large. Similar results were found when solving this problem with different input signals and different starting vectors. Figures 8 and 9 show typical results for an input vector of four sampling legs

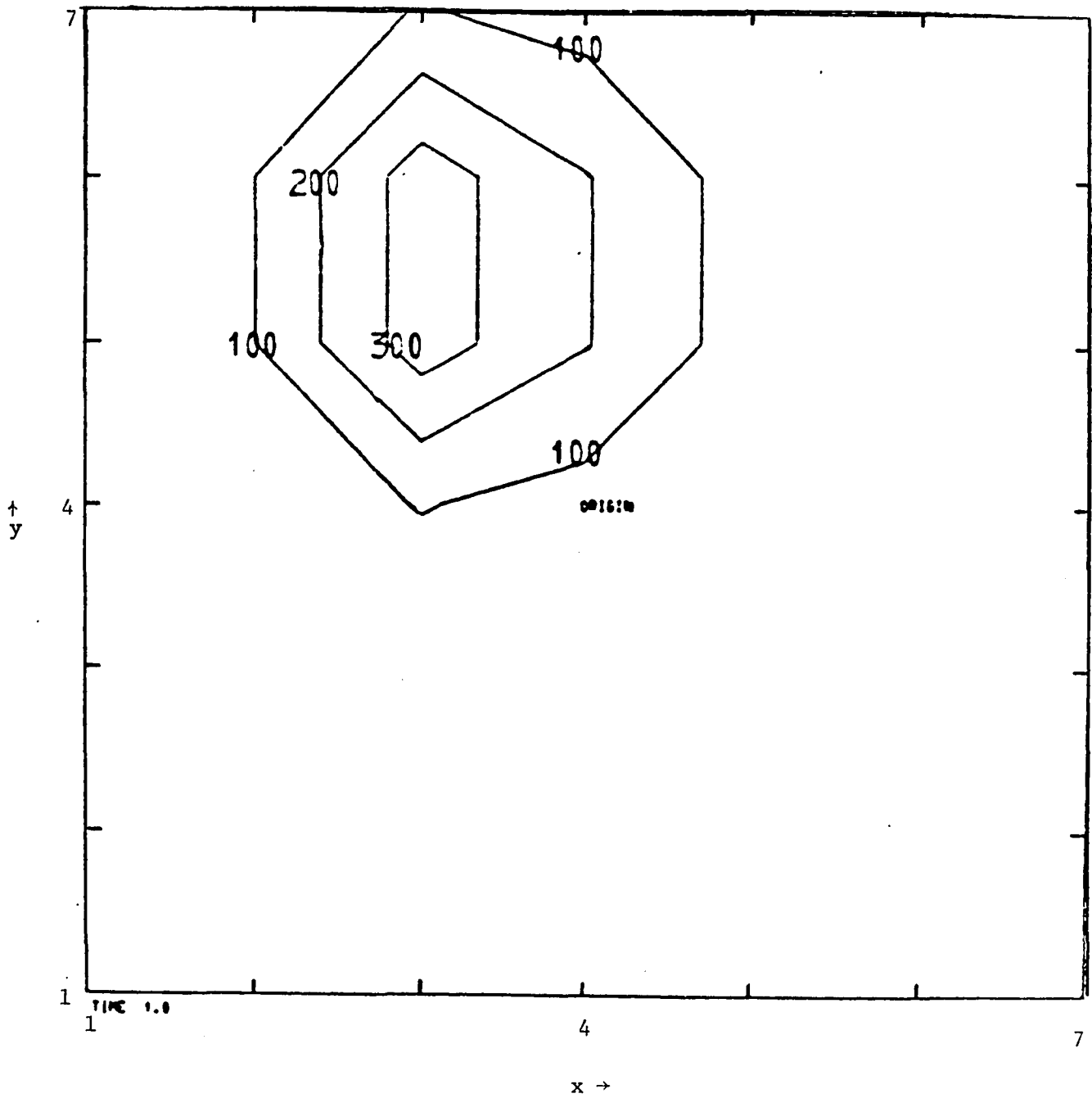


Figure 4: The expected value of the signal function, equation (6), for all $z_i = 0$, all $t_i = 1$, and $x_0, y_0, t_0 = 4., 4., 2$.

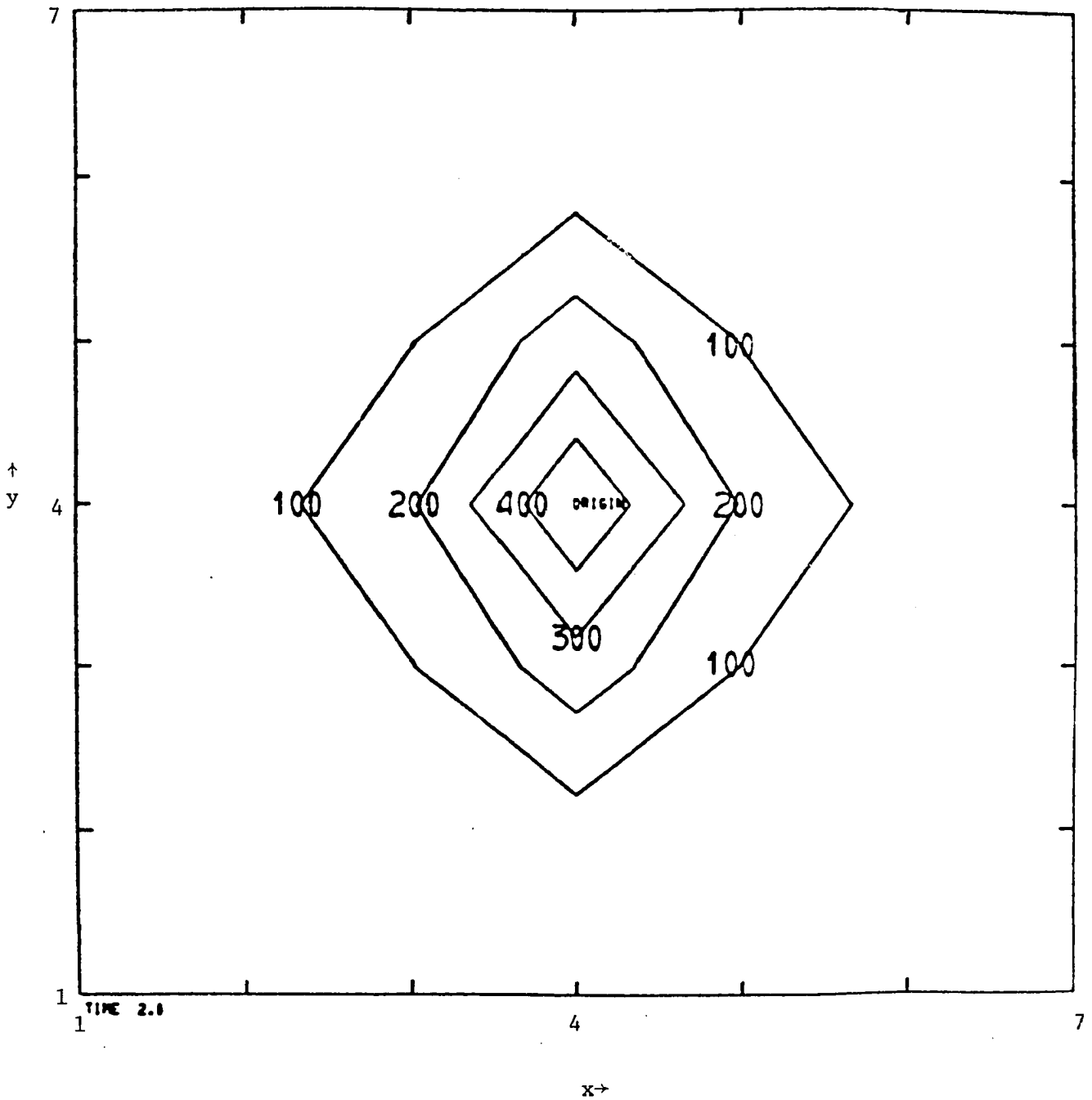


Figure 5 The expected value of the signal function, equation (6), for all $z_i = 0$, all $t_i = 2$. and $x_0, y_0, t_0 = 4., 4., 2$.

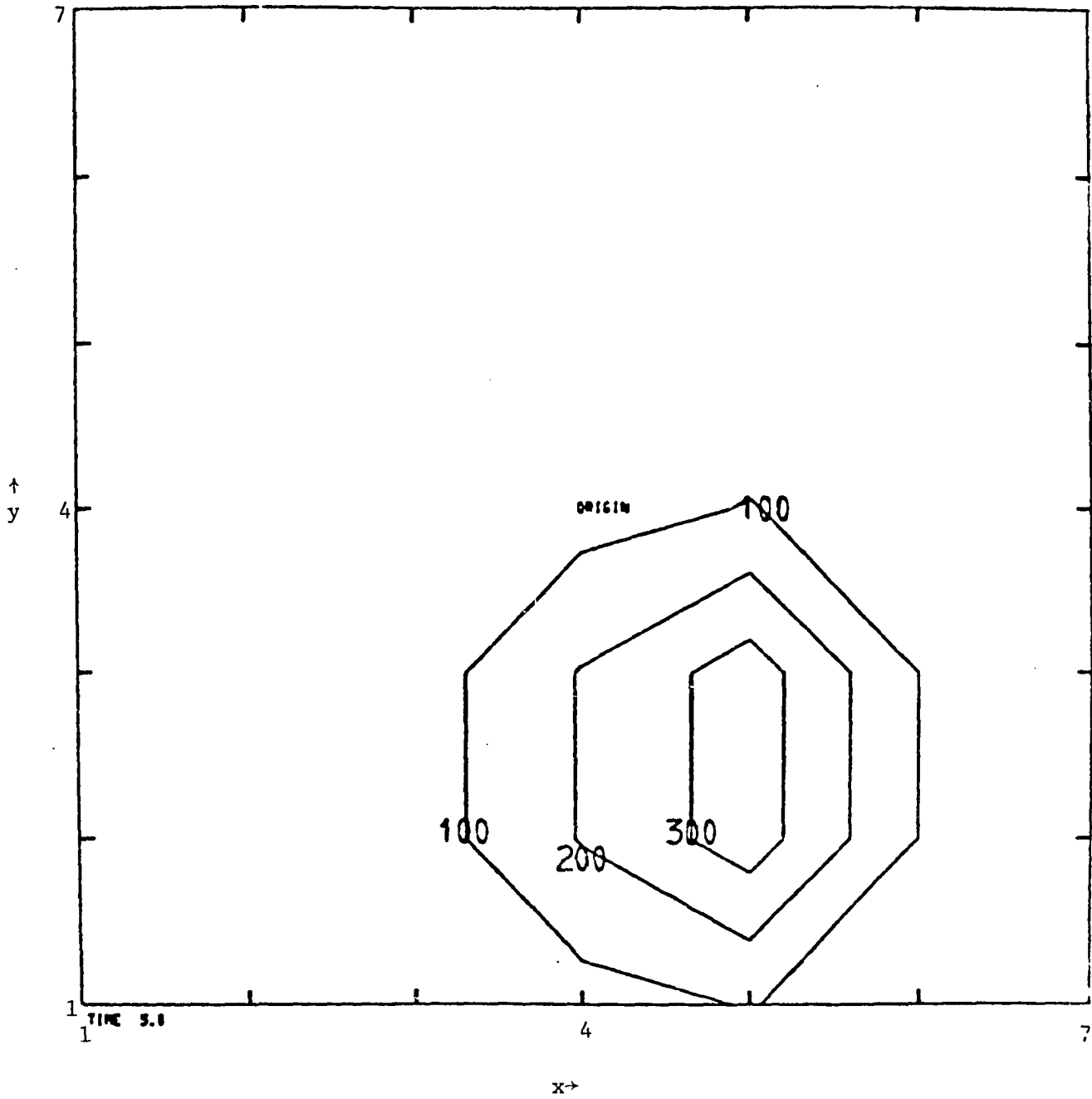


Figure 6 The expected value of the signal function, equation (6), for all $z_i = 0$, all $t_i = 3$, and $x_0, y_0, t_0 = 4., 4., 2$.

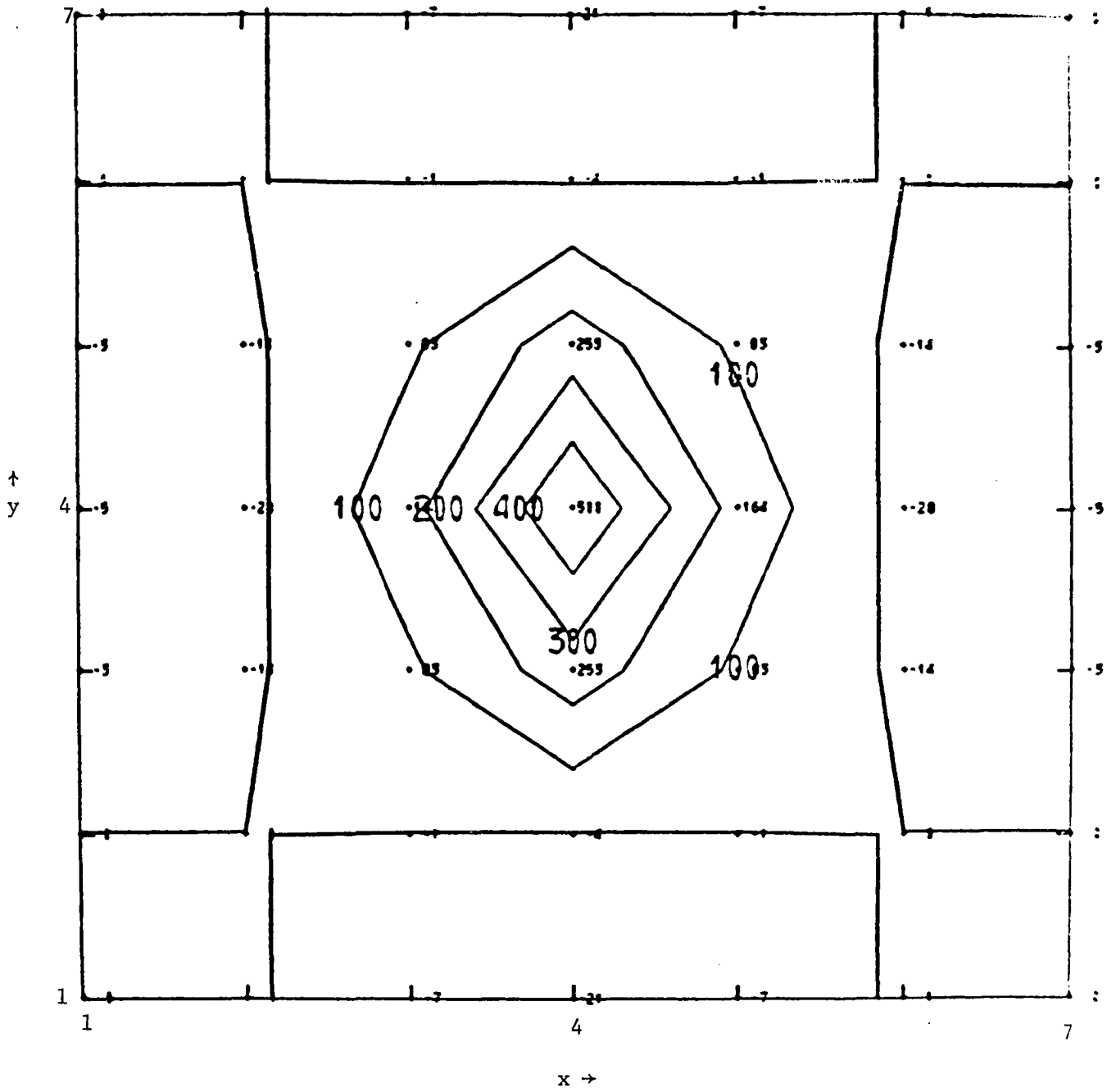


Figure 7 The true signal for all $z_i = 0$ and all $t_i = 2$ displayed on a 7x7 grid. Central value is 5.

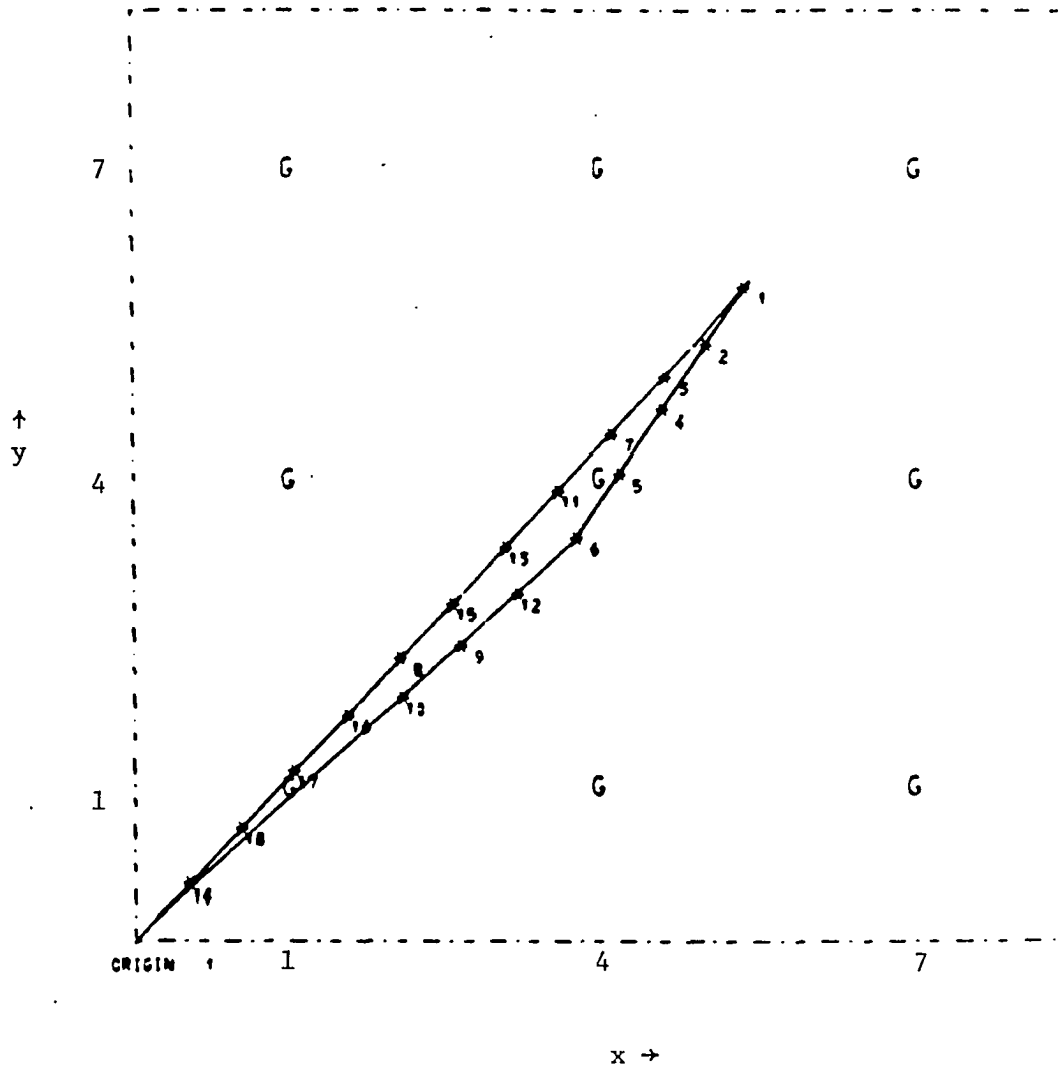


Figure 8 The optimal sensor placement for sampling when the sensors are fixed for all time. The sampling origin is $x_0, y_0 = 0., 0.$

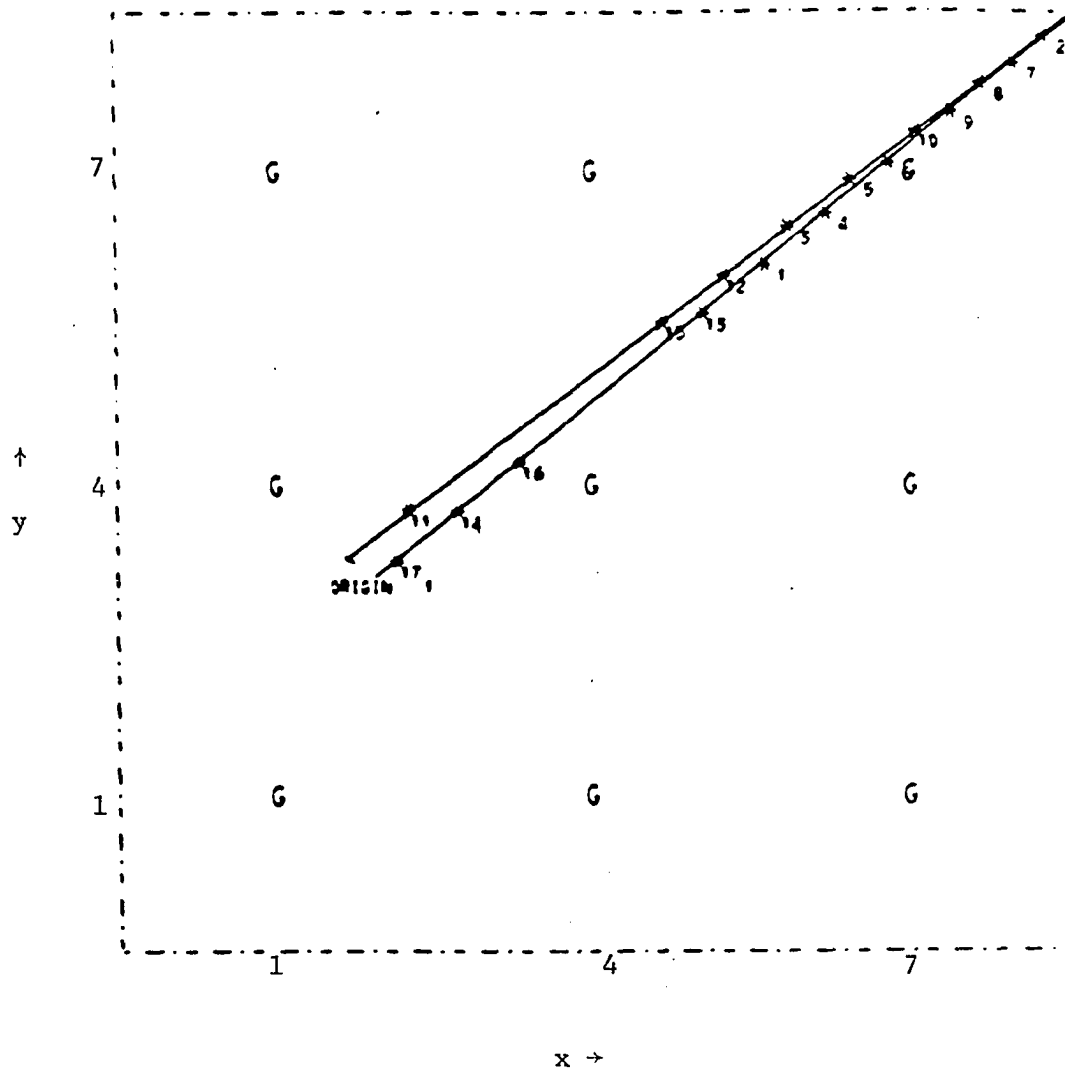


Figure 9 : The optimal sensor placement for sampling when the sensors are fixed for all time. The sampling origin is $x_0, y_0 = 1.5, 3.5$.

where the maximum number of sensors allowed was 18 and the origin of the sampling patterns are as shown. In these cases as well as others, the optimal sensor placement consists essentially of a linear arrangement of sensors which is perpendicular to the path of movement of the signal function. This is interesting in that a similar sensor placement technique (Kays, 1973) which places sensors sequentially instead of simultaneously, selected a sensor placement pattern which is along the path of the signal function.

The next set of tests run on the optimal sampling methodology involved horizontal sampling and analysis where all $z_i = 0$ and the maximum number of sensors allowed was 40. For this work, the input vector selected was as shown in figure 10. This input vector is based upon a flight pattern suggested for the Global Atmospheric Research Program's Atlantic Tropical Experiment (GATE) by Zipser, 1973. The input pattern was oriented in order that the sensing system closely followed the signal as it moved across the grid. The sample points in figure 10 show all the possible sampling locations allowed for this track. Both the first and the last sample points of each leg are not admissible.

Figures 11 and 12 show the analyses possible with this input sampling pattern for cases A and B where $\rho_1=0$ and $S/N=10$ and $S/N=1$ respectively. Figures 13 and 14 are similarly defined except that, for cases C and D, $\rho_1=.5$. A signal-to-noise ratio of 10 is used to represent a strong signal and weak noise. The signal-to-noise ratio of 1 is based on the results of an investigation by Eddy and

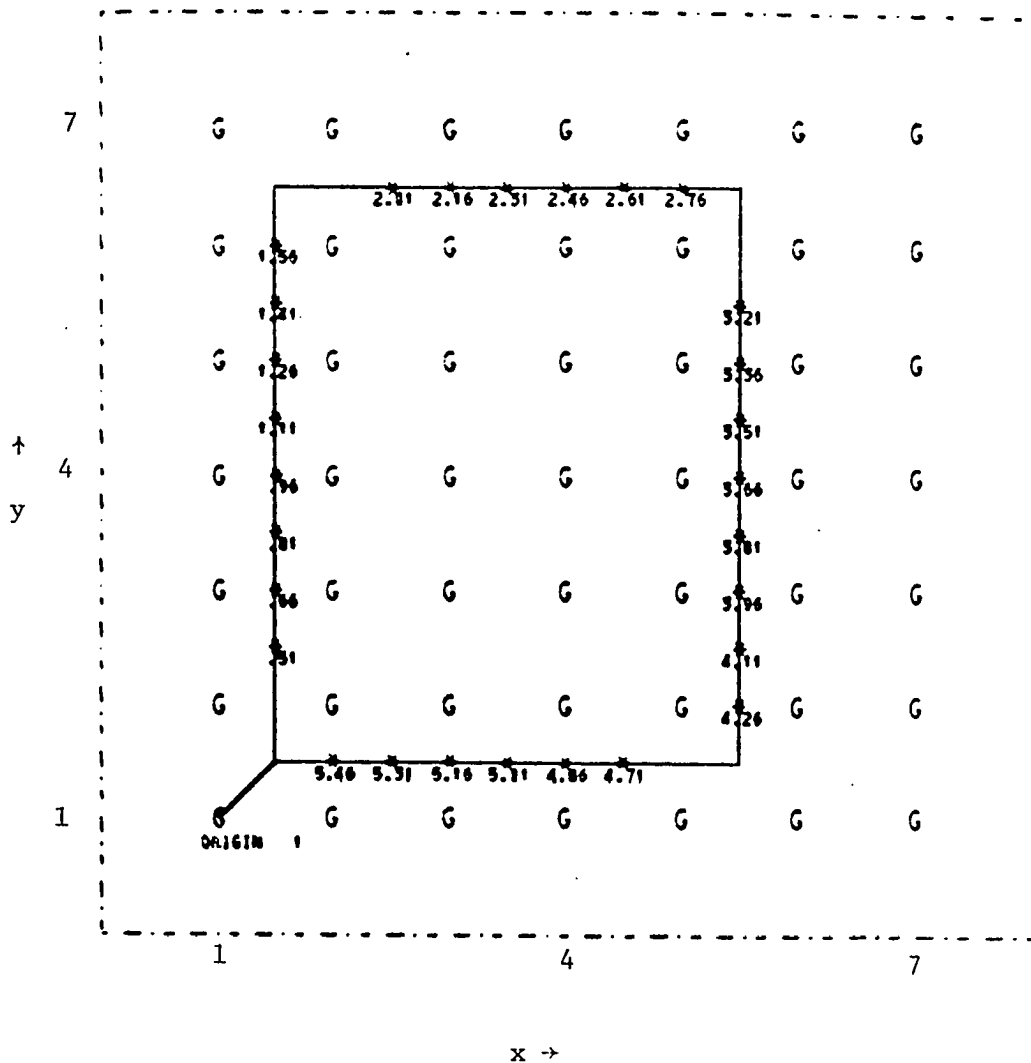


Figure 10 The sampling pattern used as input to the optimization algorithm in order to sample the signal shown in figures 4 through 6 in order to analyze the true signal (figure 7). All possible sample points are shown.

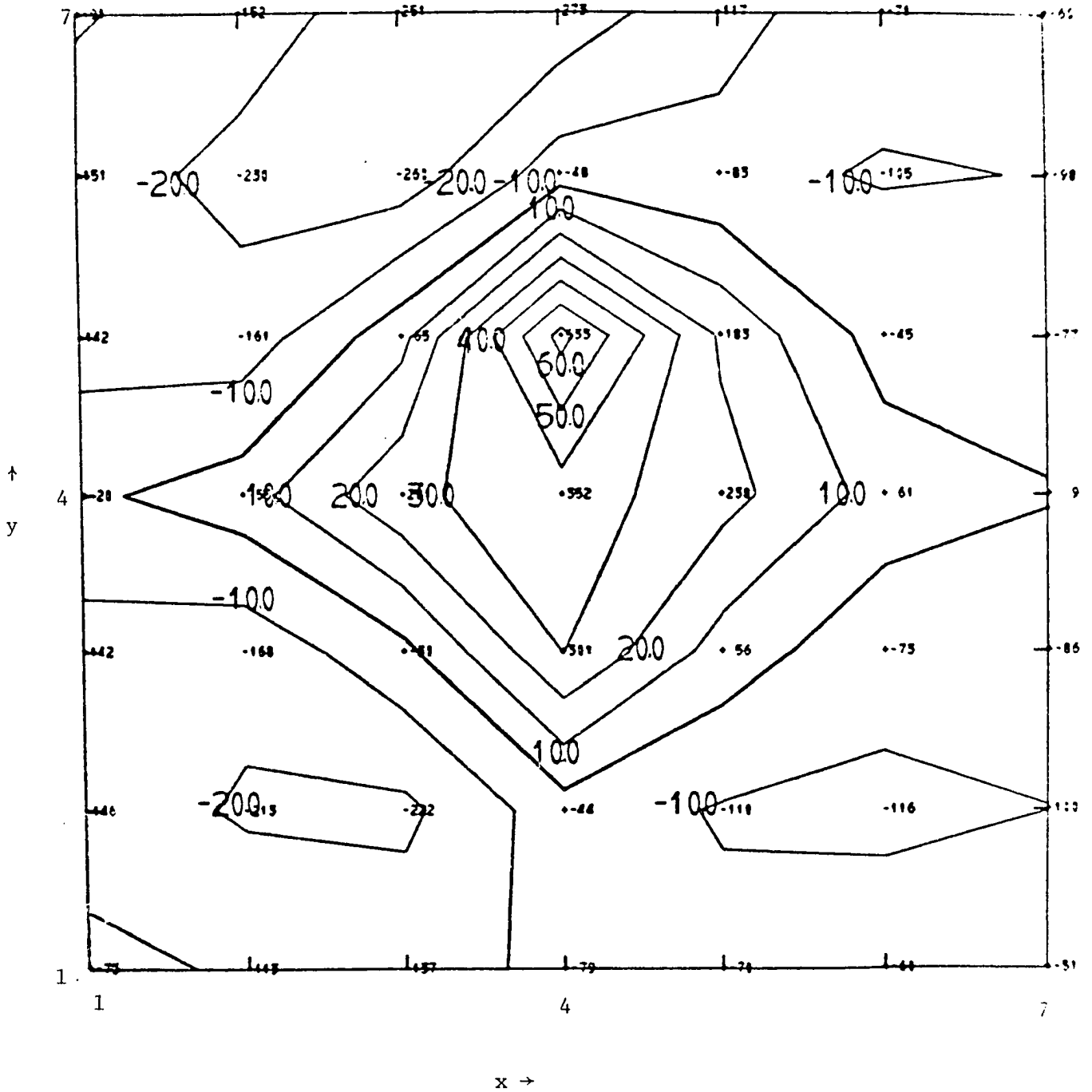


Figure 12: Case B - An objective analysis available using the sample points of the input vector for $S/N = 1.$ and $\rho_1 = 0.$

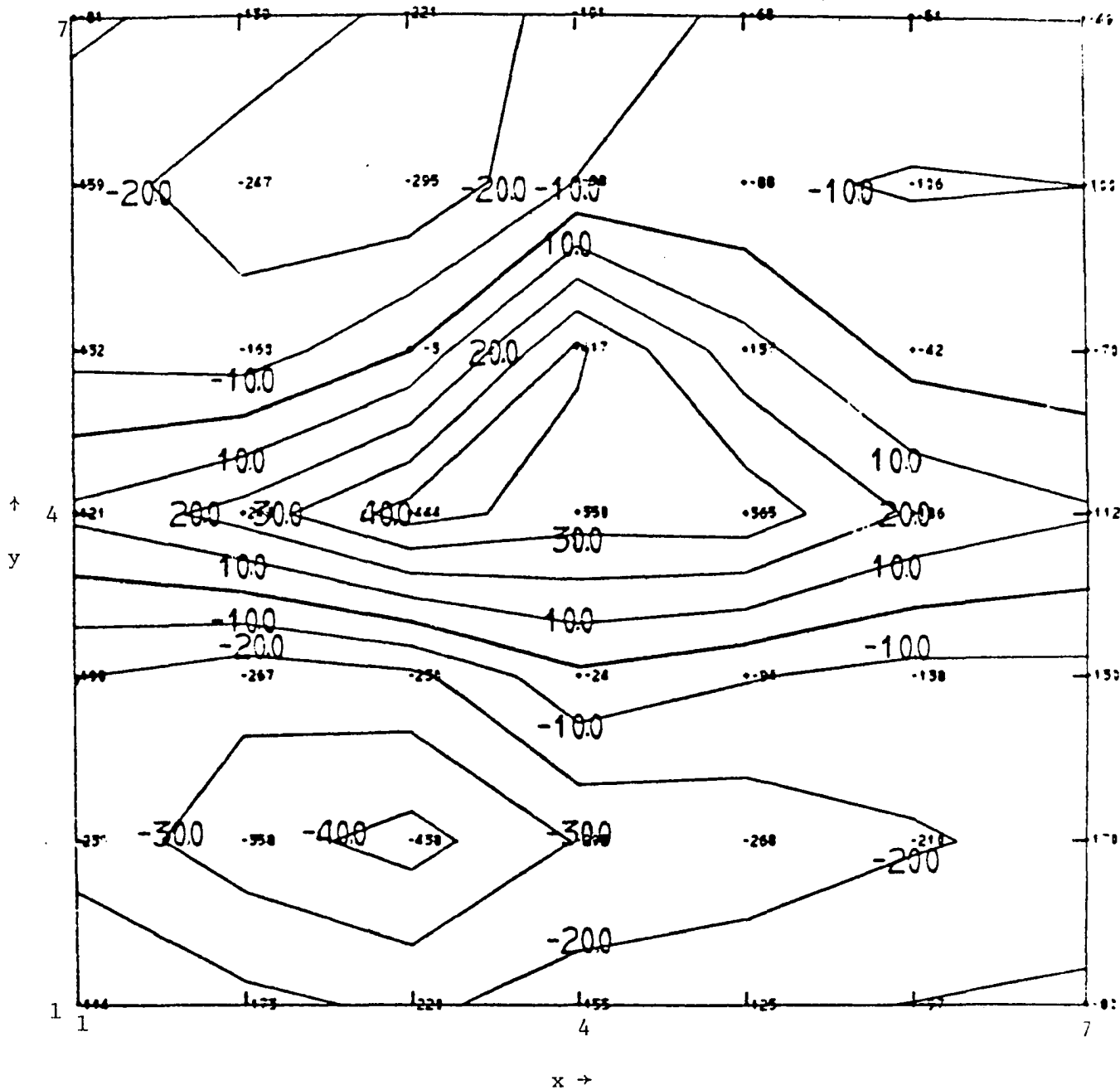


Figure 14: Case D - An objective analysis available using the sample points of the input vector for $S/N = 1.$ and $\rho_1 = .5$

Rose (1973) into the analysis of a known divergence-convergence pattern using a data set of sampled winds.

Figures 15 through 18 show the optimal flight tracks selected by the optimal sampling algorithm for cases A through D. Figures 19 through 22 show the resulting objective analyses possible with these revised flight patterns. In every case, the objective analysis after the flight track adjustment by the optimization process is better than is attainable with the input sampling pattern. Both of the objective analyses for each case were conducted using the true covariance function of the input signal along with the signal values from equation (5) and a set of randomized noise values corresponding to the specified signal-to-noise ratio. Therefore, any deterioration in the objective analyses resulting from inaccuracies in the covariance definition should affect both analyses similarly.

Table 1 shows the amount of unexplained variance along with the average root-mean-square value over the grid for the objective analysis done before and after the optimization process. The number of sensors allowed was 40 although no sampling configuration used more than 30. The criterion for the use of an additional sensor was that it explain more than .1% of the unexplained variance over the grid.

Figure 23 shows the effect of increasing the signal-to-noise ratio for the sampling on the amount of unexplained variance over the grid for both the input and the optimum solution vector. The values plotted are a result of using the single input vector shown in figure 10.

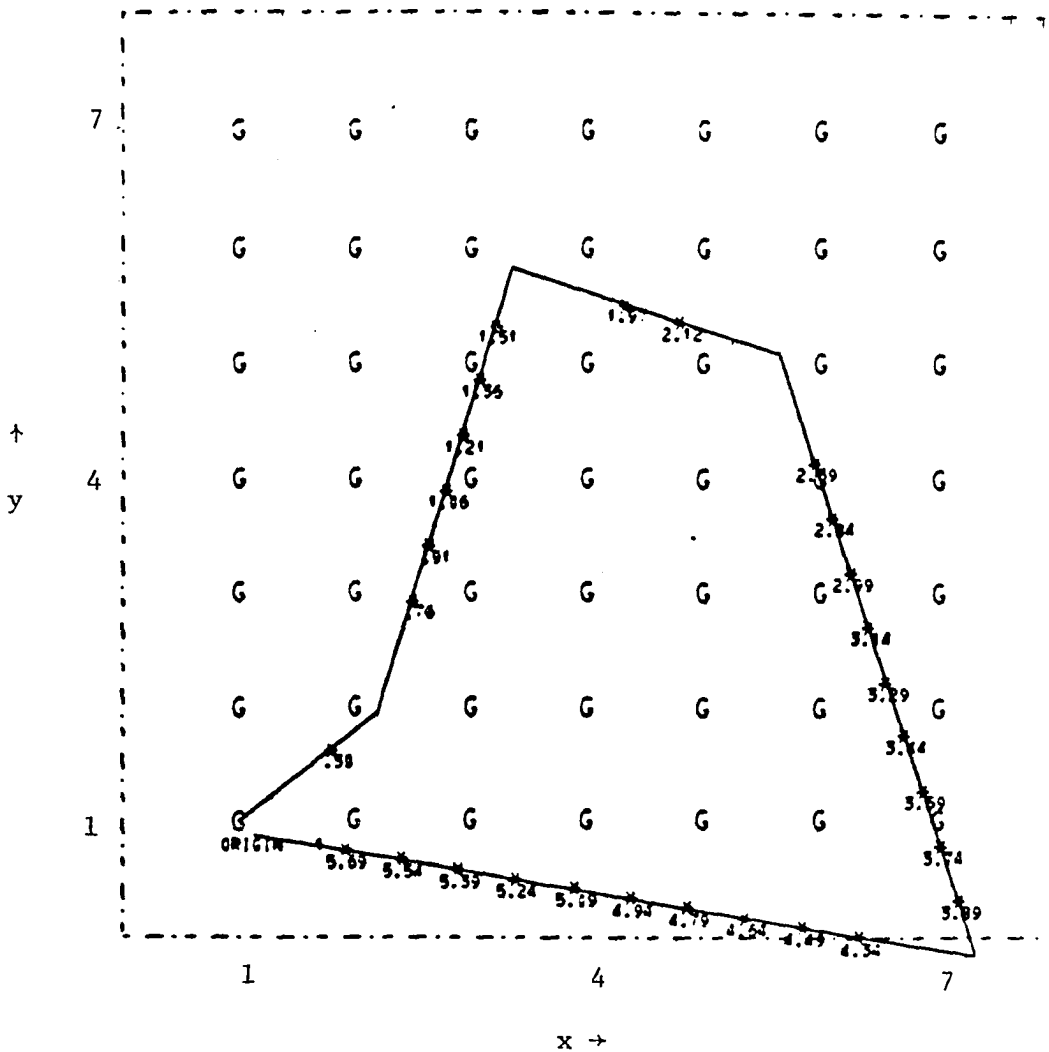


Figure 15: Case A -The optimal flight path and sampling locations computed by the optimization algorithm for $S/N = 10$ and $\rho_1 = 0$.

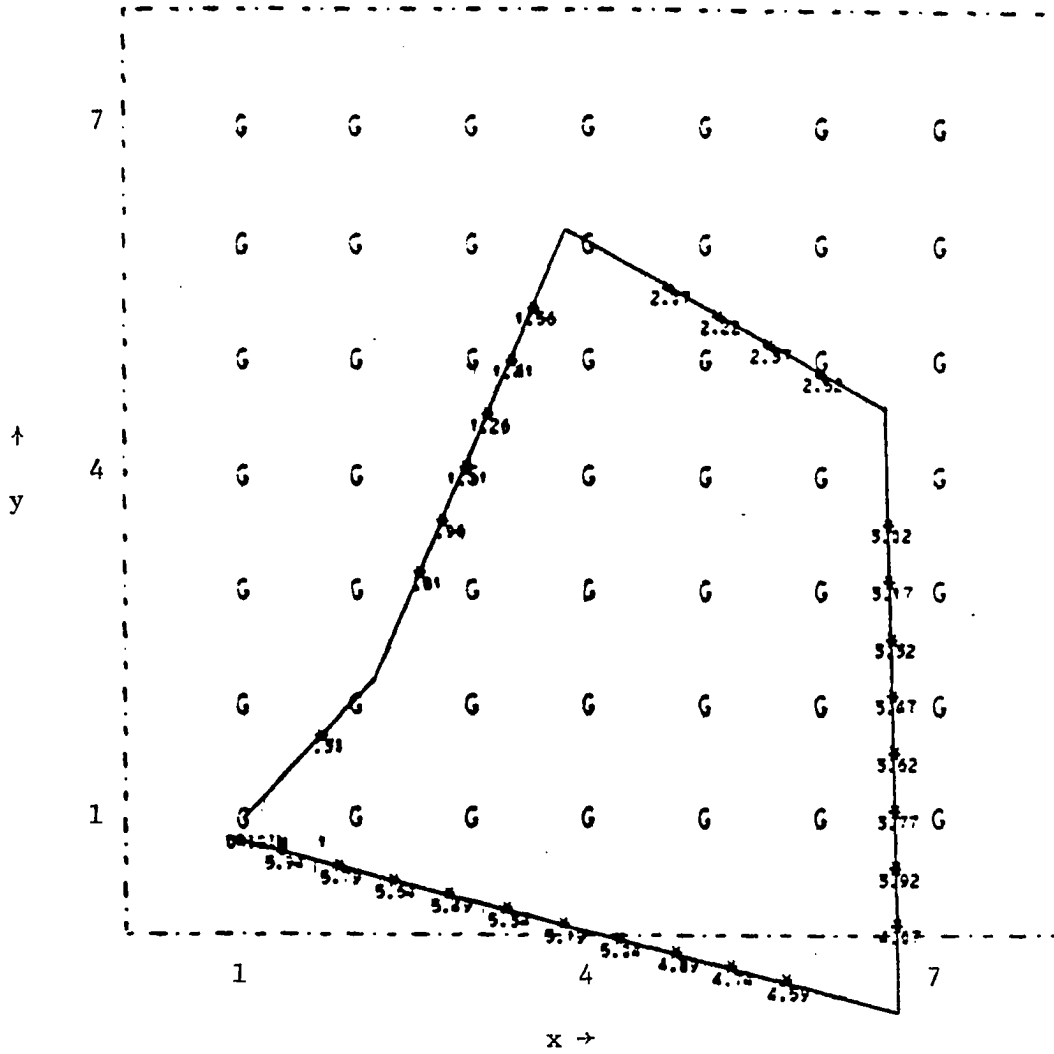


Figure 17: Case C - The optimal flight path and sampling locations computed by the optimization procedure for $S/N = 10$. and $\rho_1 = .5$

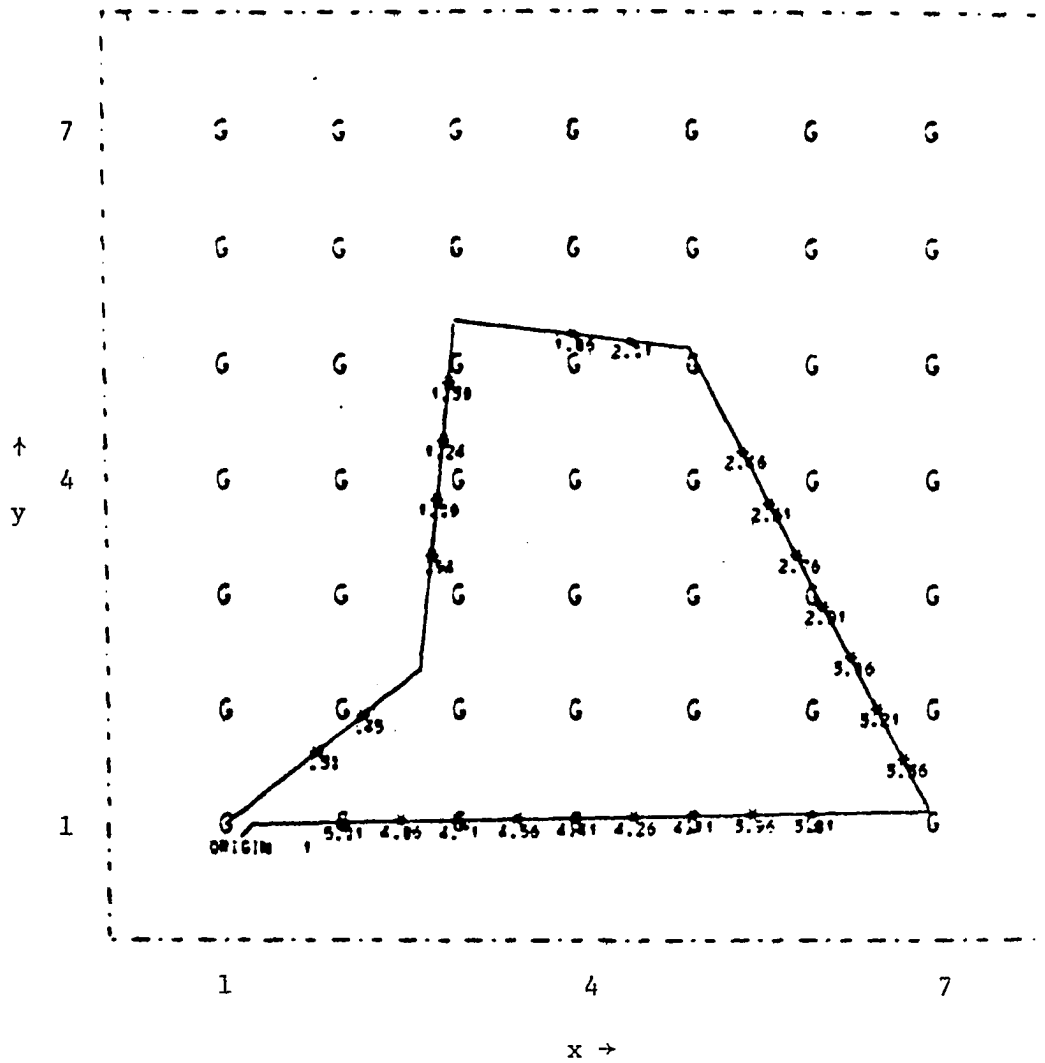


Figure 18: Case D - The optimal flight path and sampling locations computed by the optimization algorithm for $S/N = 1.$ and $\rho_1 = .5$

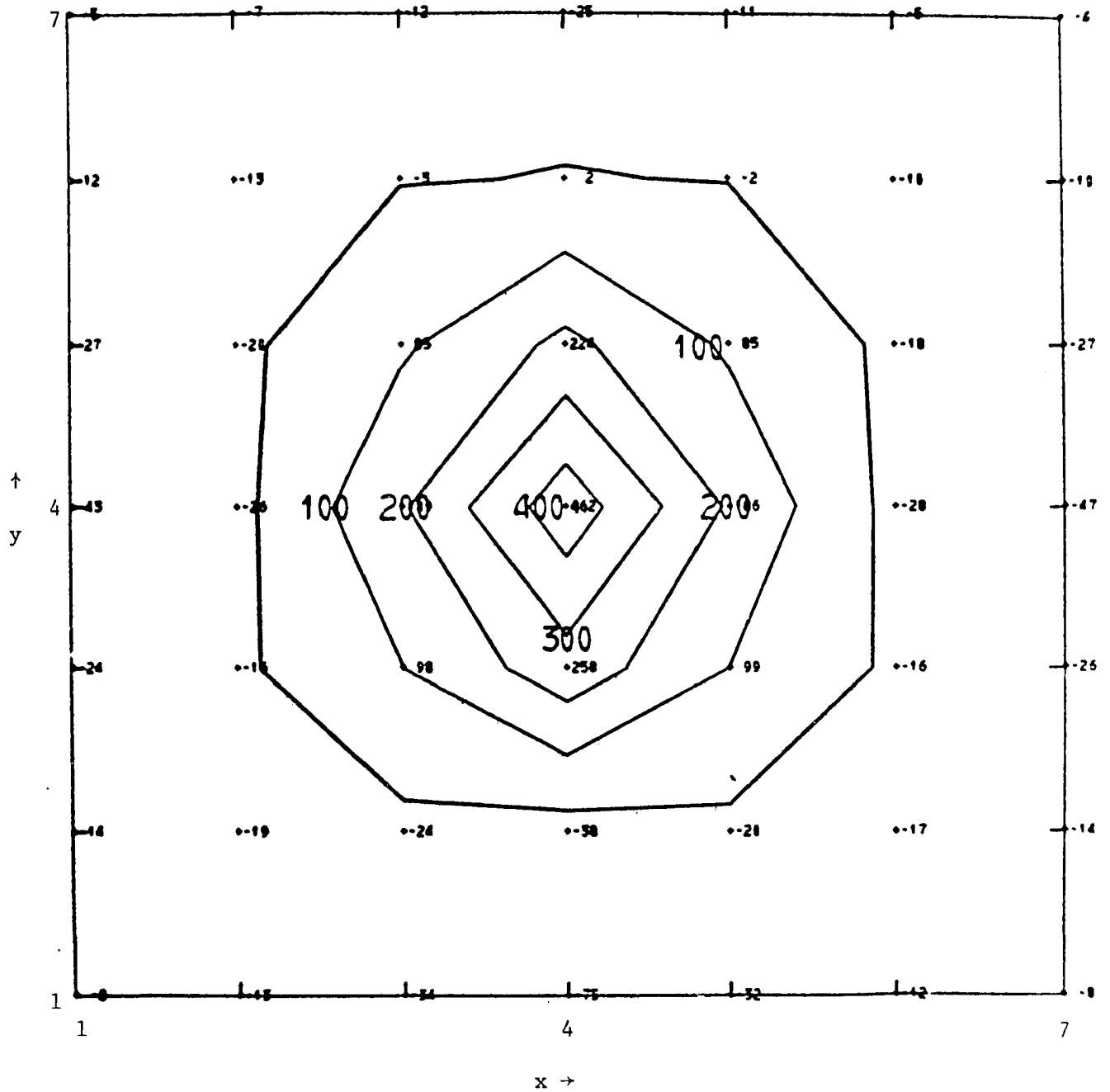


Figure 19: Case A - An objective analysis using the sample points available along the optimal flight track for $S/N = 10$ and $\rho_1 = 0$.

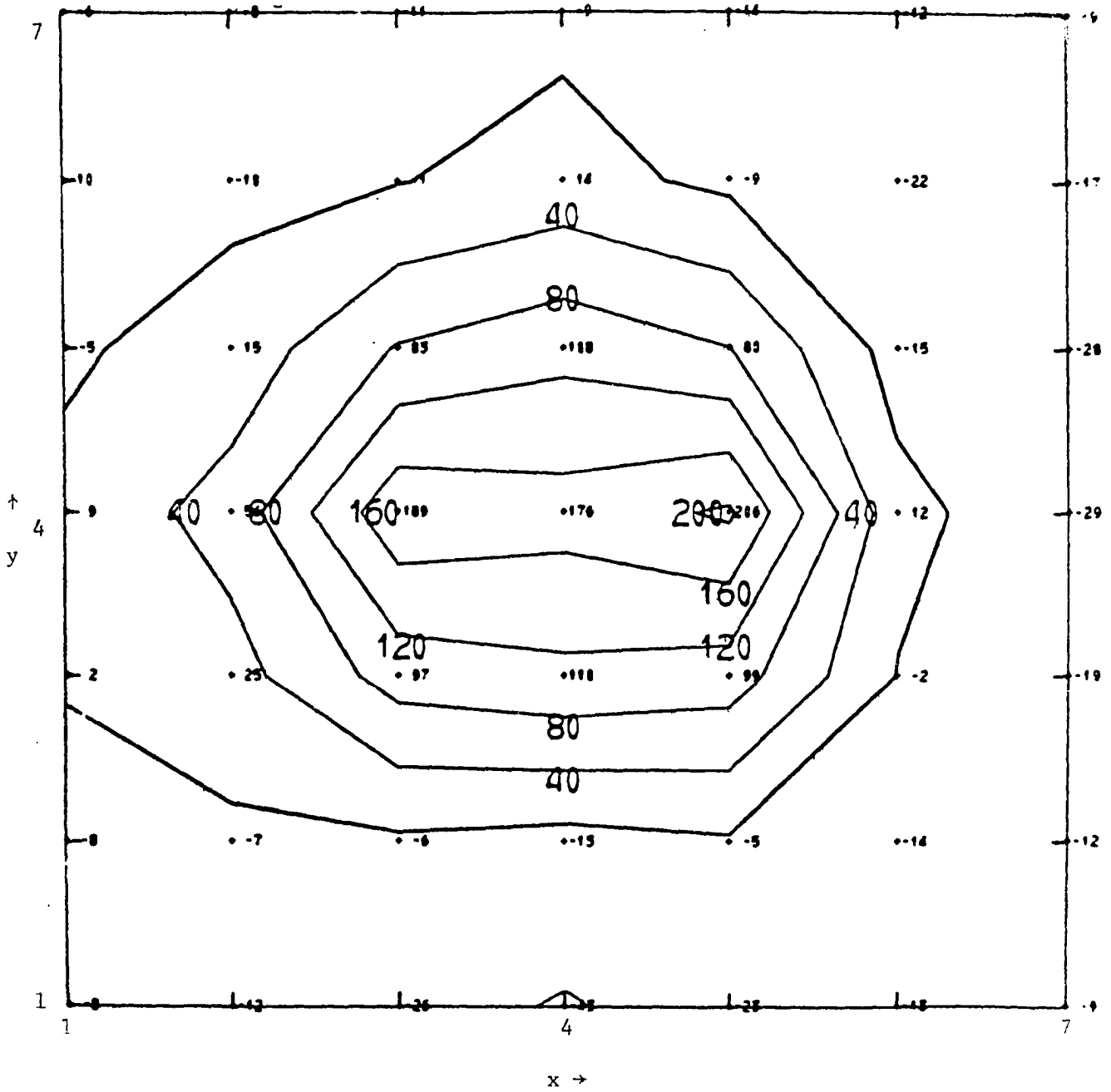


Figure 20: Case B - An objective analysis using the sample points available along the optimal flight path for $S/N = 1$, and $\rho_1 = 0$.

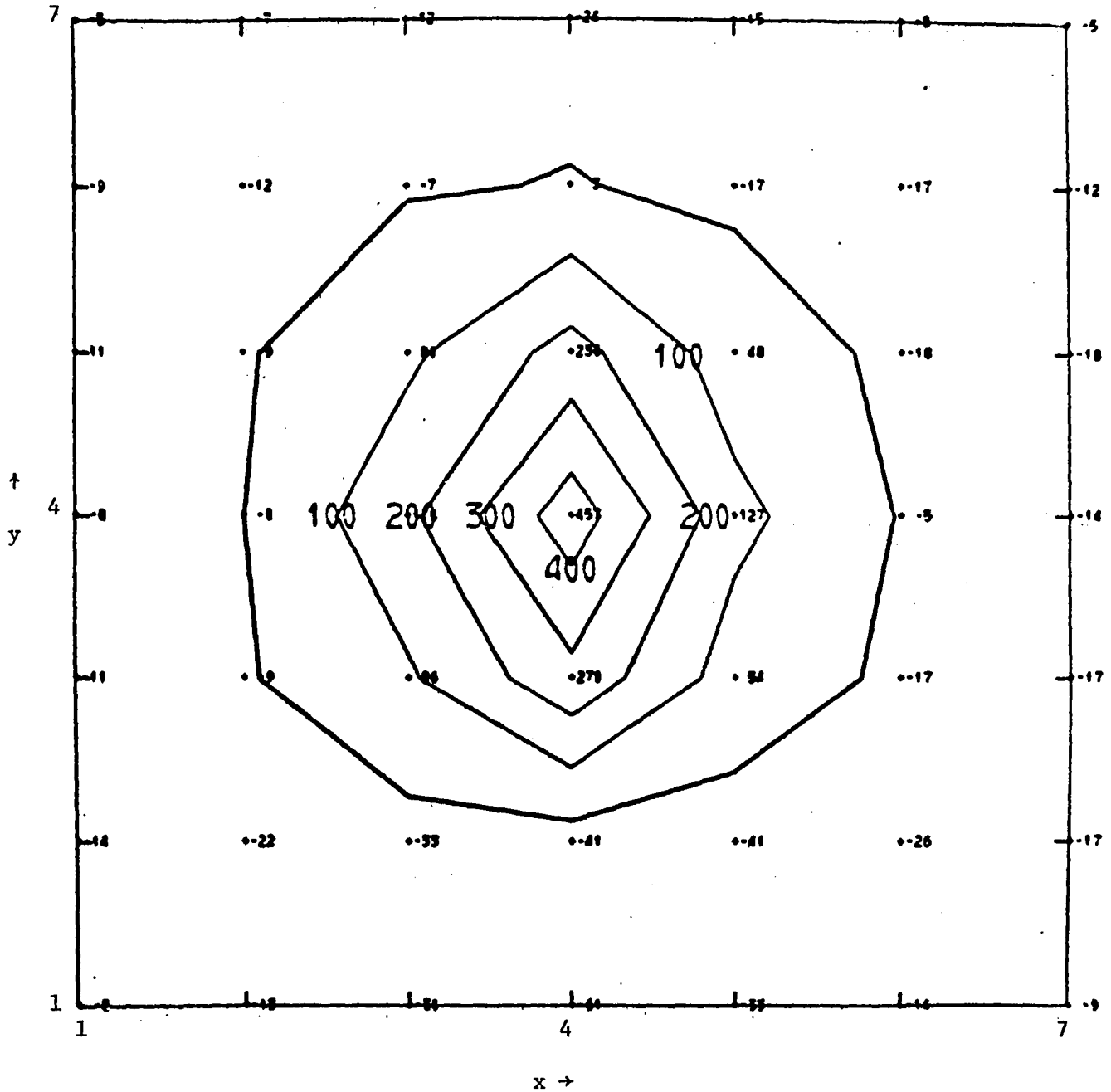


Figure 21: Case C - An objective analysis using the sample points available along the optimal flight track for $S/N = 10$ and $\rho_1 = .5$

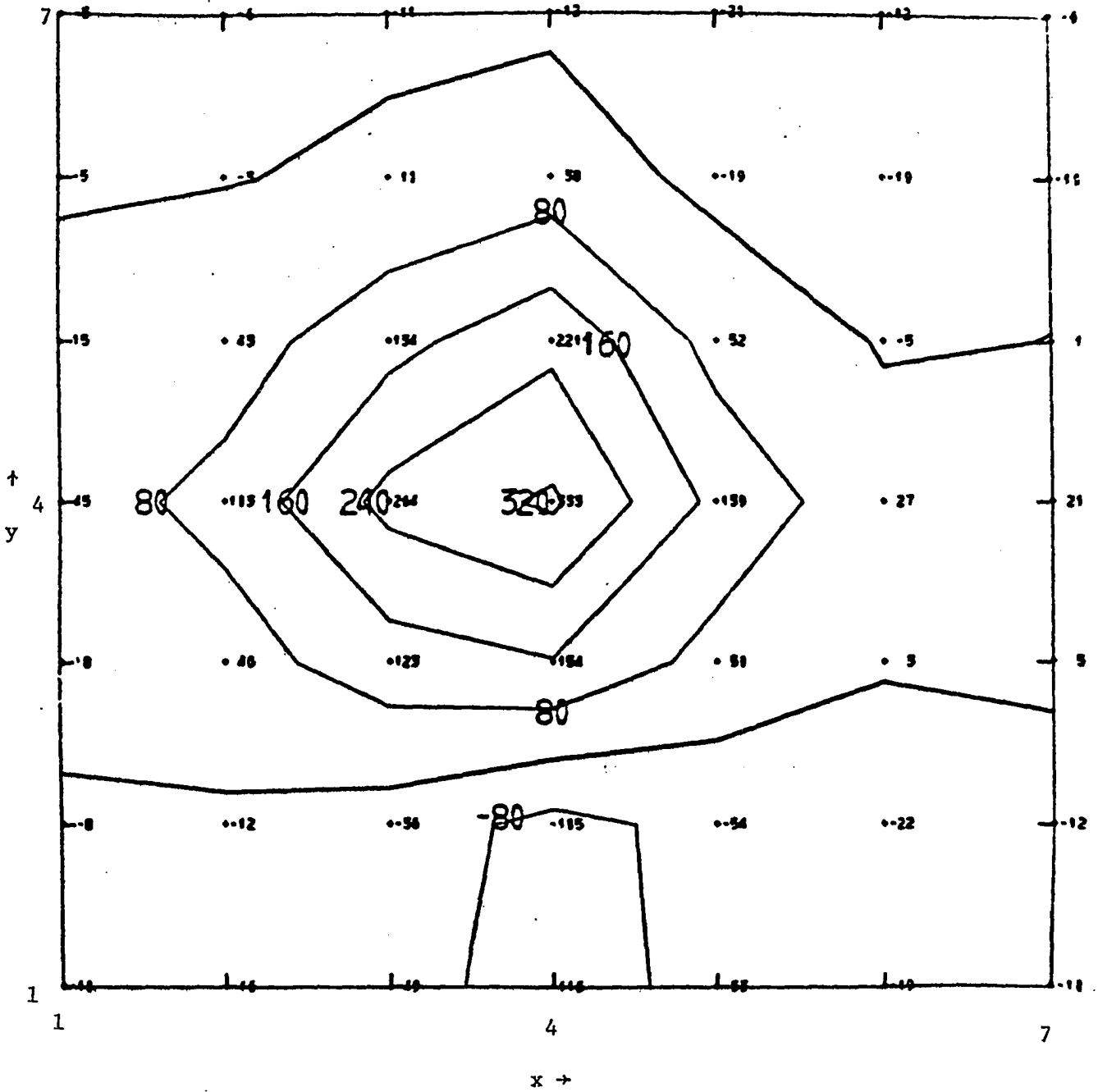


Figure 22: Case D - An objective analysis using the sampling points available along the optimal flight path for $S/N = 1$. and $\rho_1 = .5$

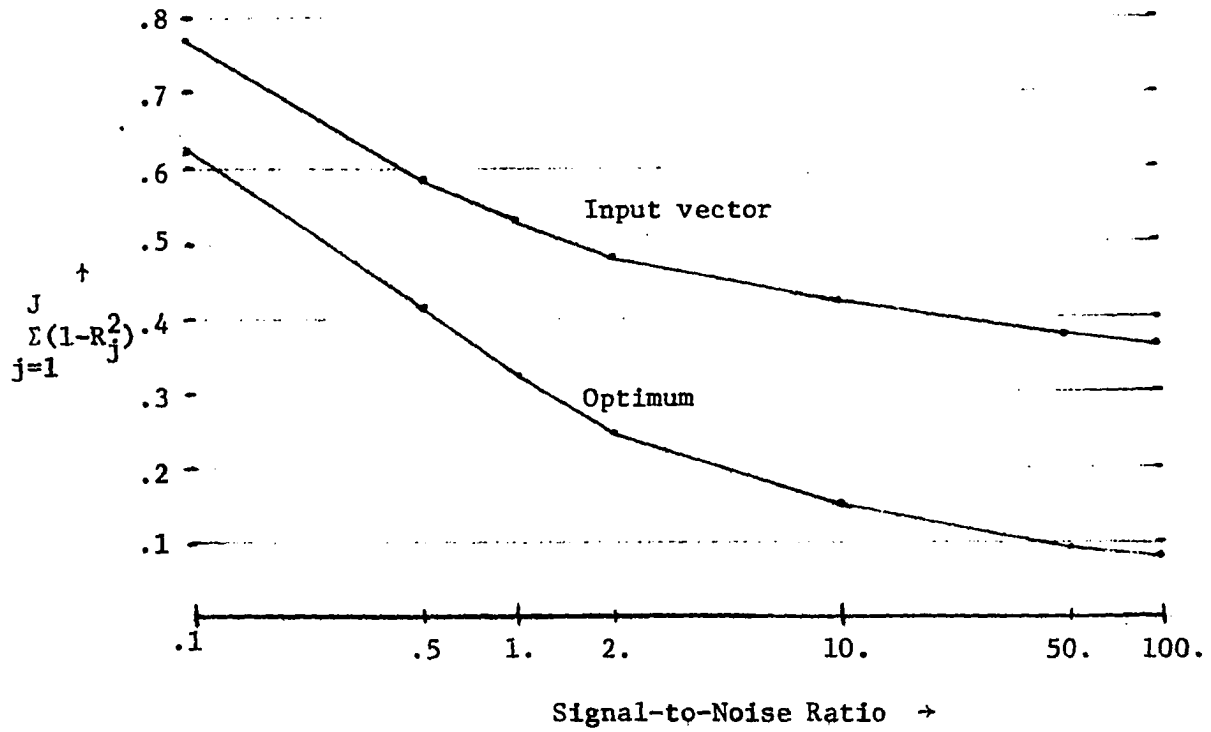


Figure 23: A comparison of the unexplained variance over the grid for the input vector and the optimal solution for various signal-to-noise ratios.

		$\sum_{j=1}^J (1-R_j^2)$	$\overline{\text{RMS}}$	Number of Sensors Used
CASE A :	Input	.420	.485	28
	Optimum	.154	.037	28
CASE B :	Input	.534	.756	28
	Optimum	.322	.341	29
CASE C :	Input	.419	.491	28
	Optimum	.143	.038	29
CASE D :	Input	.548	.824	27
	Optimum	.307	.245	24

TABLE 1

Number of sensors allowed	Input	Optimum	
6	.430 (6)	.227 (6)	
10	.398 (10)	.129 (10)	S/N = 50
20	.381 (20)	.099 (20)	
40	.379 (28)	.098 (28)	$\rho_1 = 0.$

TABLE 2

Table 2 provides the values for the unexplained variance when the number of sensors is restricted. The actual number of sensors used by each solution (initial and optimum) is shown in parentheses. Using this table, figure 23 and a value system for unexplained variance over the grid, a decision is possible as to the number and quality of the instruments needed to accomplish research goals.

A scale size test was run which first doubled and then, halved the input signal wavelengths in the x and y directions for a $S/N=50$ and $\rho_1=0$. For the large scale size, the unexplained variance between the input vector and the optimum showed only slight improvement from .025 to .003. However, for the small scale size, an improvement from .661 to .166 was obtained. An in-depth study of the relationship between analysis grid, scale size of sampled phenomenon and the accuracy of the variance-covariance definition is still necessary before a definitive statement on the applicability to a specific problem is possible. Figure 24 and 26 show the suggested flight tracks for sampling the large and small scale signal in order to obtain an optimal signal analysis as shown in figures 25 and 27.

Another test of the optimization procedure was to include more than one aircraft in the sampling scheme. Input vectors for 2 and 3 sampling aircraft were placed in the space-time volume in an effort to saturate the analysis grid with observations. For 2 aircraft with $S/N=.5$ and $\rho_1=0$, the optimal solution with 30 sample points produced an unexplained variance of .326 and with 45 sample points, it was .307. In each case, the improvement over the input vector was about .2. Figures 28 and 29 show the input vector for a case of

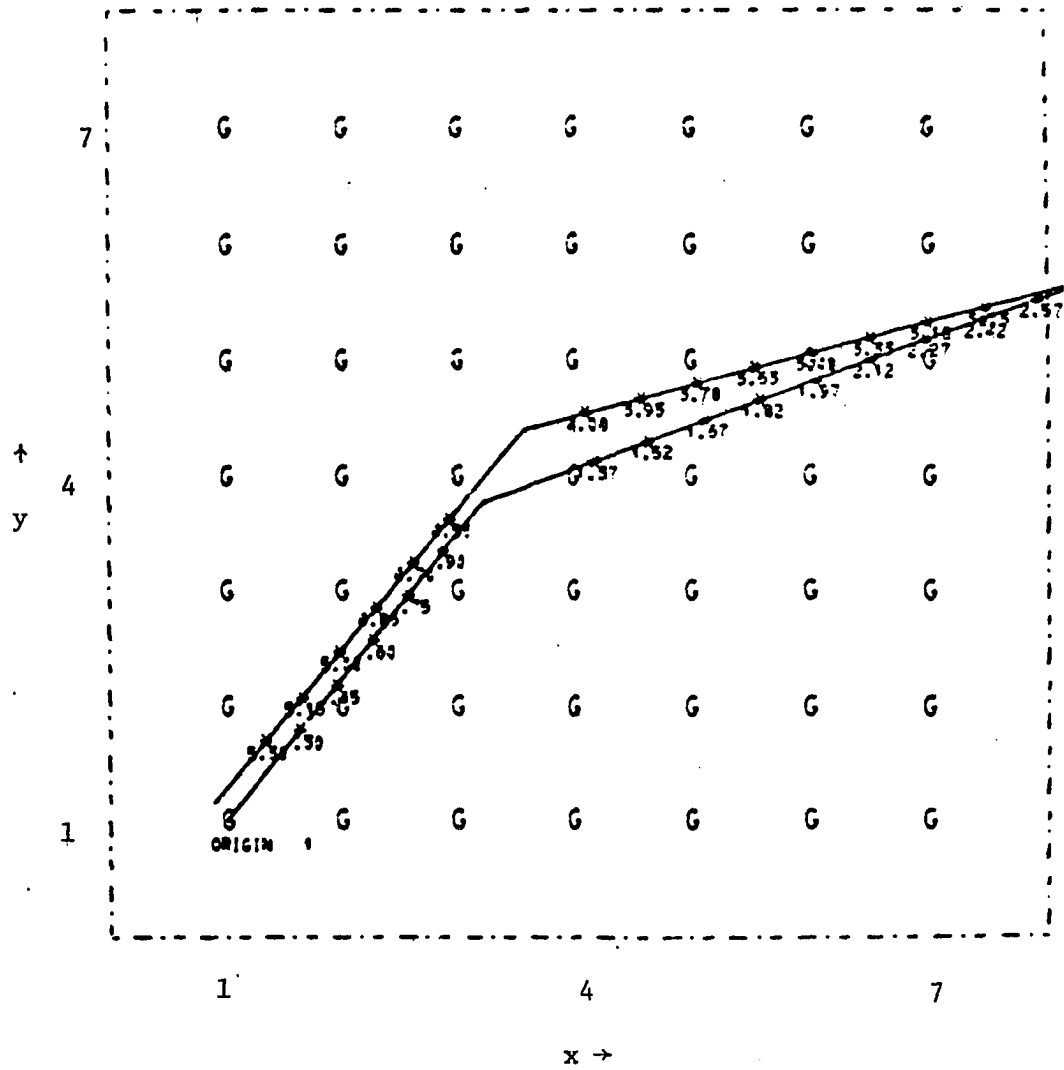


Figure 24: The optimal flight path and sampling positions computed by the optimization algorithm for a large scale signal.

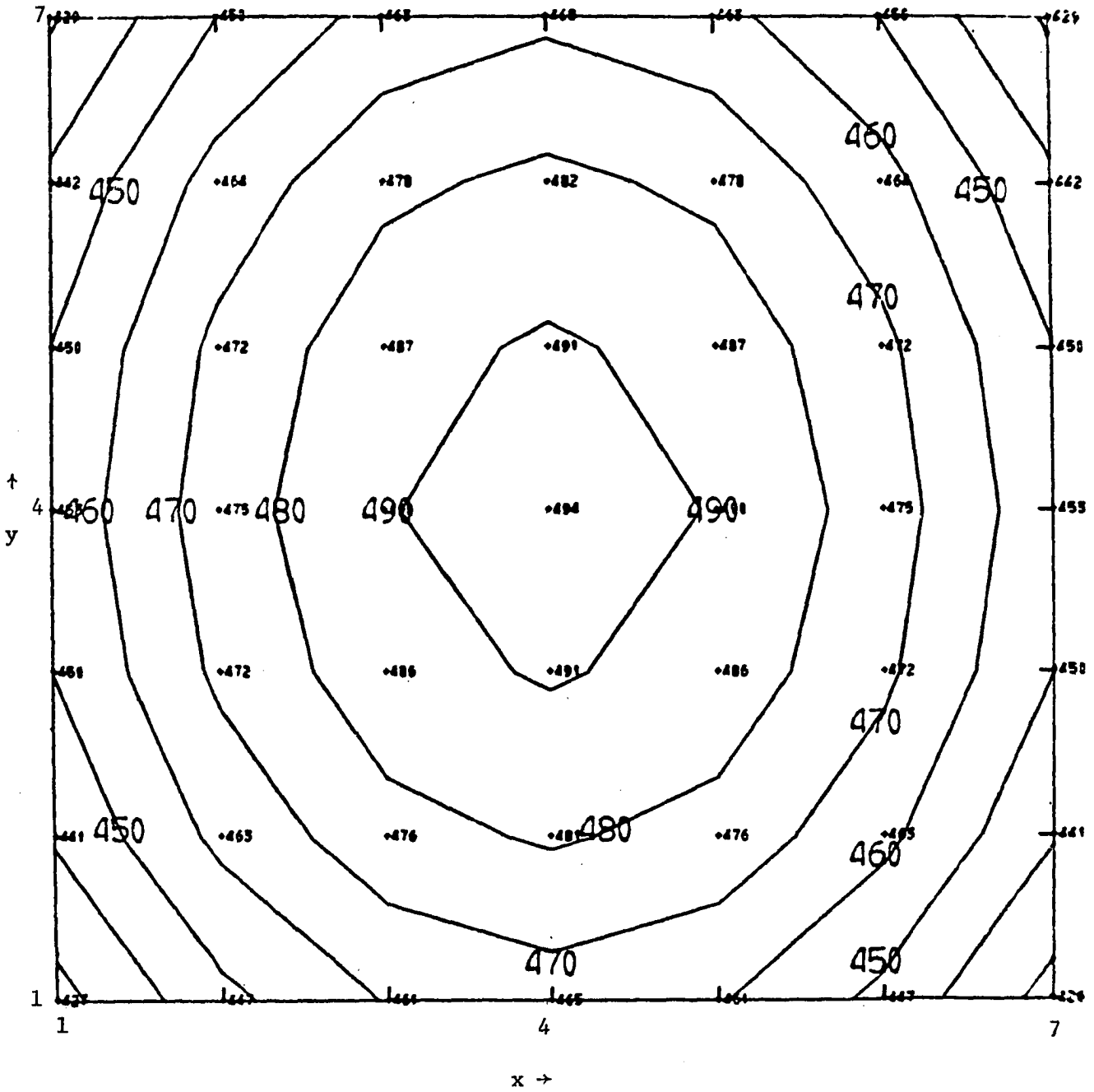


Figure 25: An objective analysis using the sample points available along the flight path shown in figure 24.

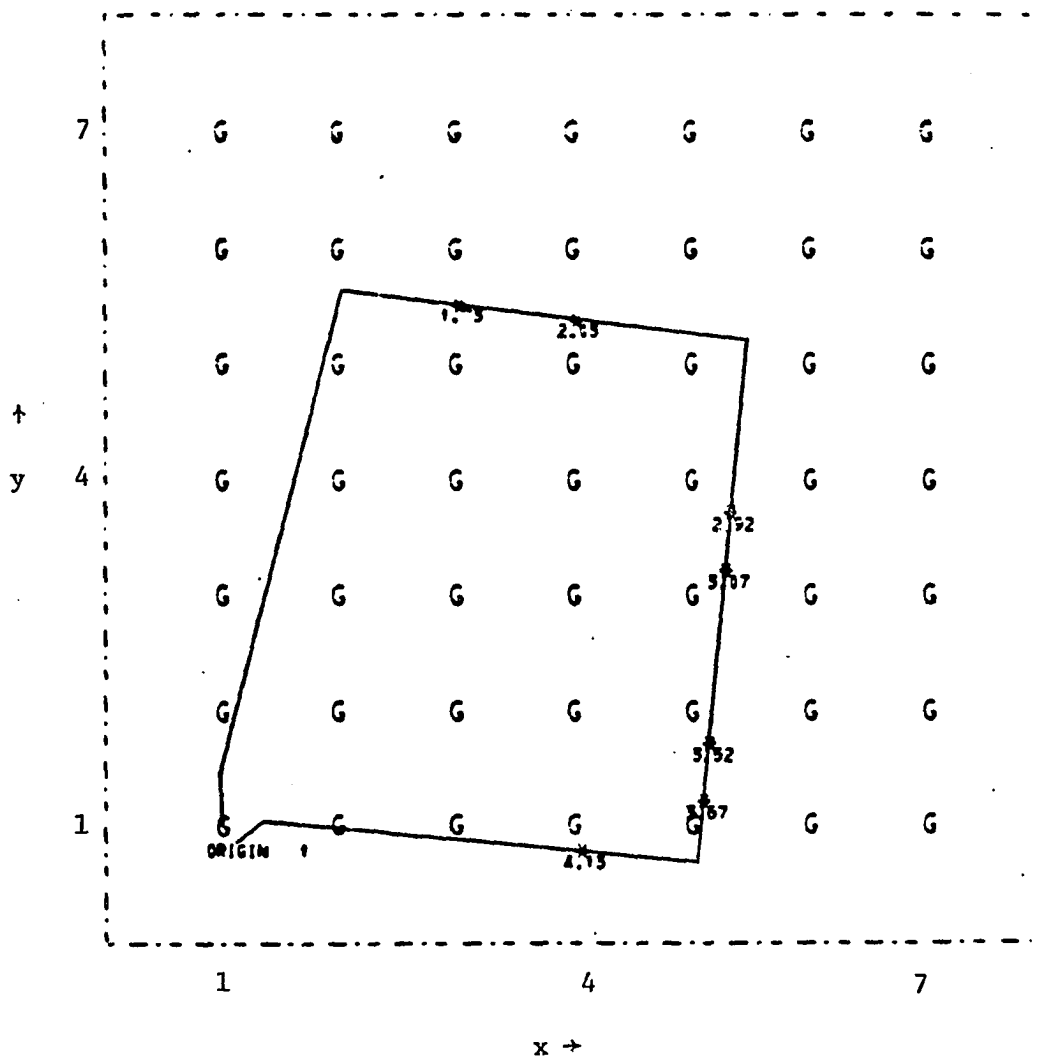


Figure 26 The optimal flight path and sampling positions computed by the optimization algorithm for a small scale signal.

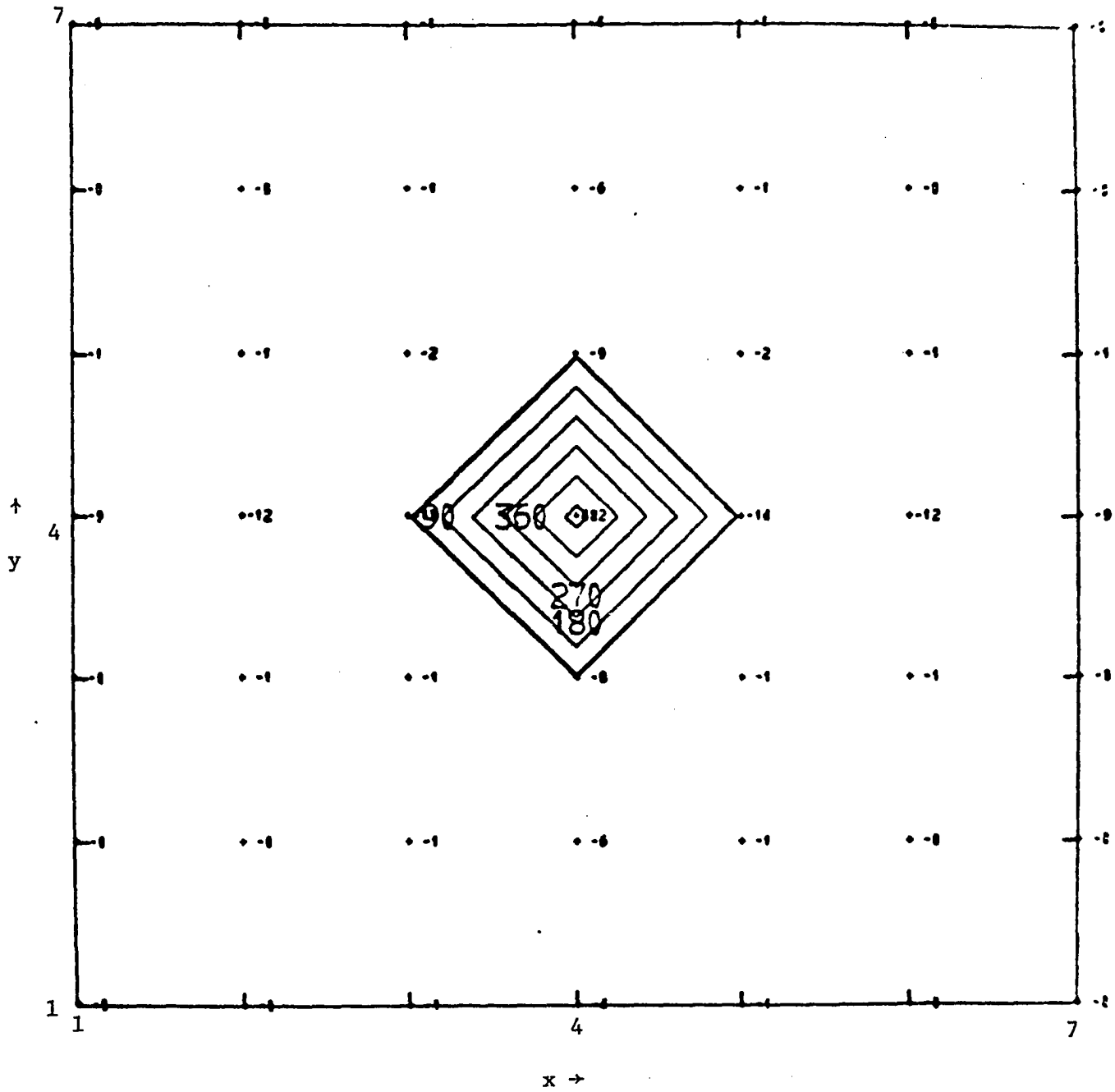


Figure 27: An objective analysis using the sample points available along the flight path shown in figure 26.

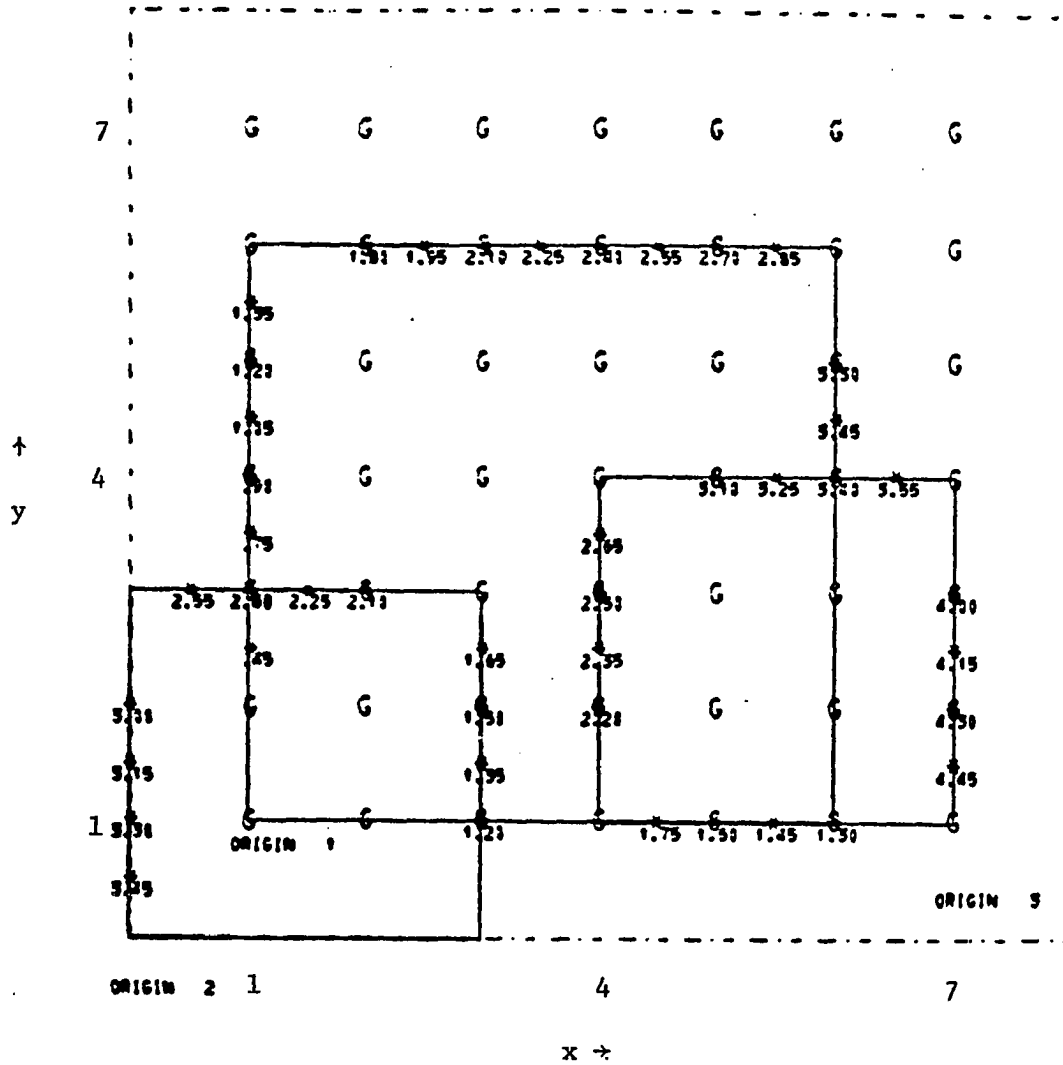


Figure 28: The input vector for the problem of using 3 aircraft to sample the atmospheric signal function of figures 4 through 6.

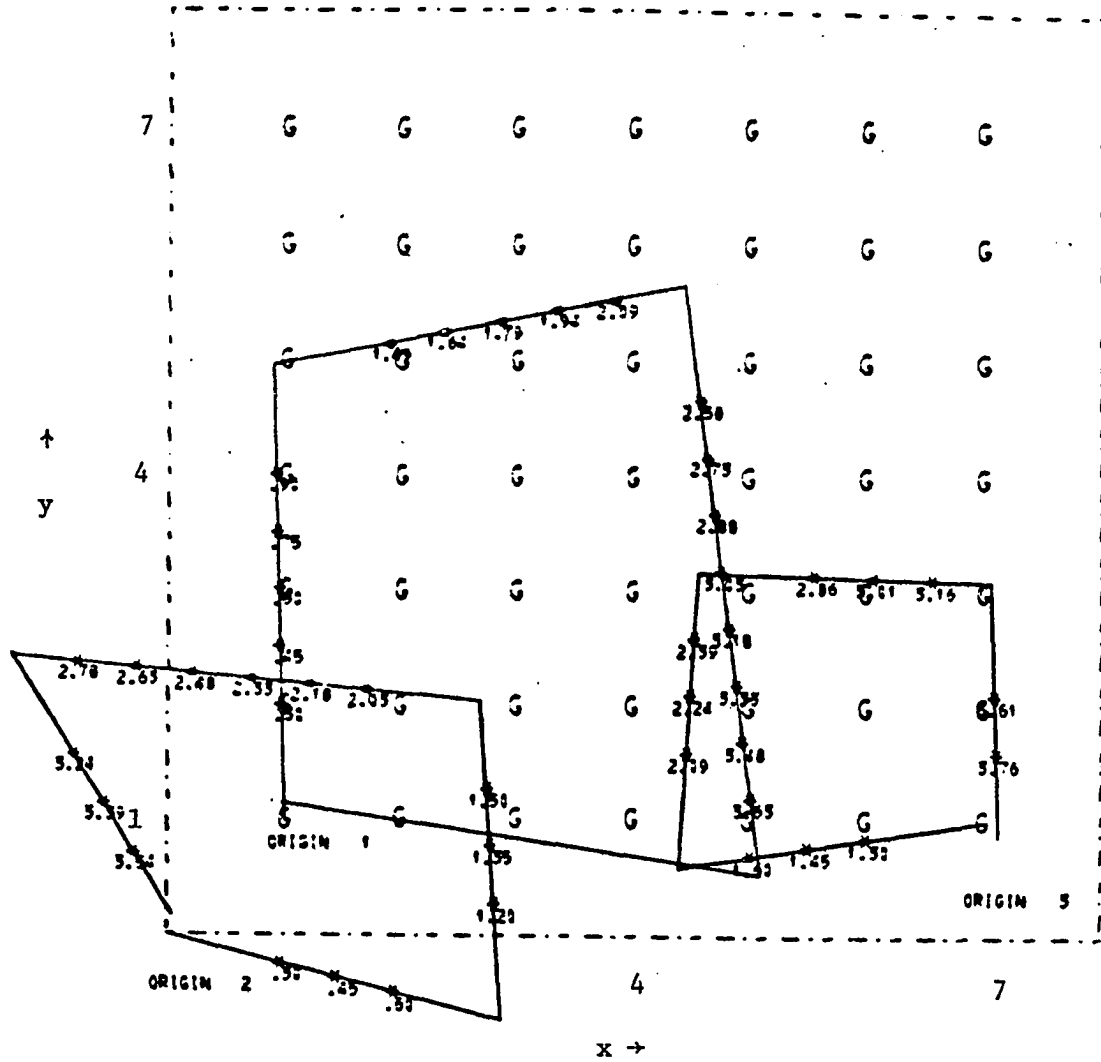


Figure 29: The optimal solution flight patterns suggested by the optimization process for the input vector of figure 28.

3 aircraft and the optimal use of those 3 aircraft as suggested by the optimization algorithm. The change in unexplained variance went from .267 to .177 and the $\overline{\text{RMS}}$ went from .339 to .112 for the objective analysis of the simulated data.

Figures 30 through 32 show the values of the objective function for twelve feasible input vectors and the resulting solution vectors from the optimization algorithm for $S/N = 100, 10$ and 1 , respectively. For $S/N = 100$, the range of the values of the objective function for the solution vectors is .024; for $S/N = 10$, the range is .057; for $S/N = 1$, the range is .070. The spread in the solution values of the objective function for $S/N = 100$ is not great enough to warrant resolving the optimization problem several times. However, when the signal-to-noise ratio is on the order of 10 or less, the optimization problem should be resolved for different input vectors and the most optimal of all these should be used for sampling.

The illustrations thus far have been for aircraft flying at a constant level. Since the z dimension will now be included, the analysis grid has been changed. The 49 grid points have been placed in the vertical with $y_i=4$ and $t_i=2$ for all i . For the signal parameters described in the beginning of this chapter, the true signal analysis for the vertical grid (where z ranges from 1 to 3) is shown in figure 33.

Figures 34 and 36 show an input and optimal flight track while figures 35 and 37 show the optimal signal analysis possible from the two tracks respectively. For this case, $S/N=1$ and $\rho_1=0$ resulting

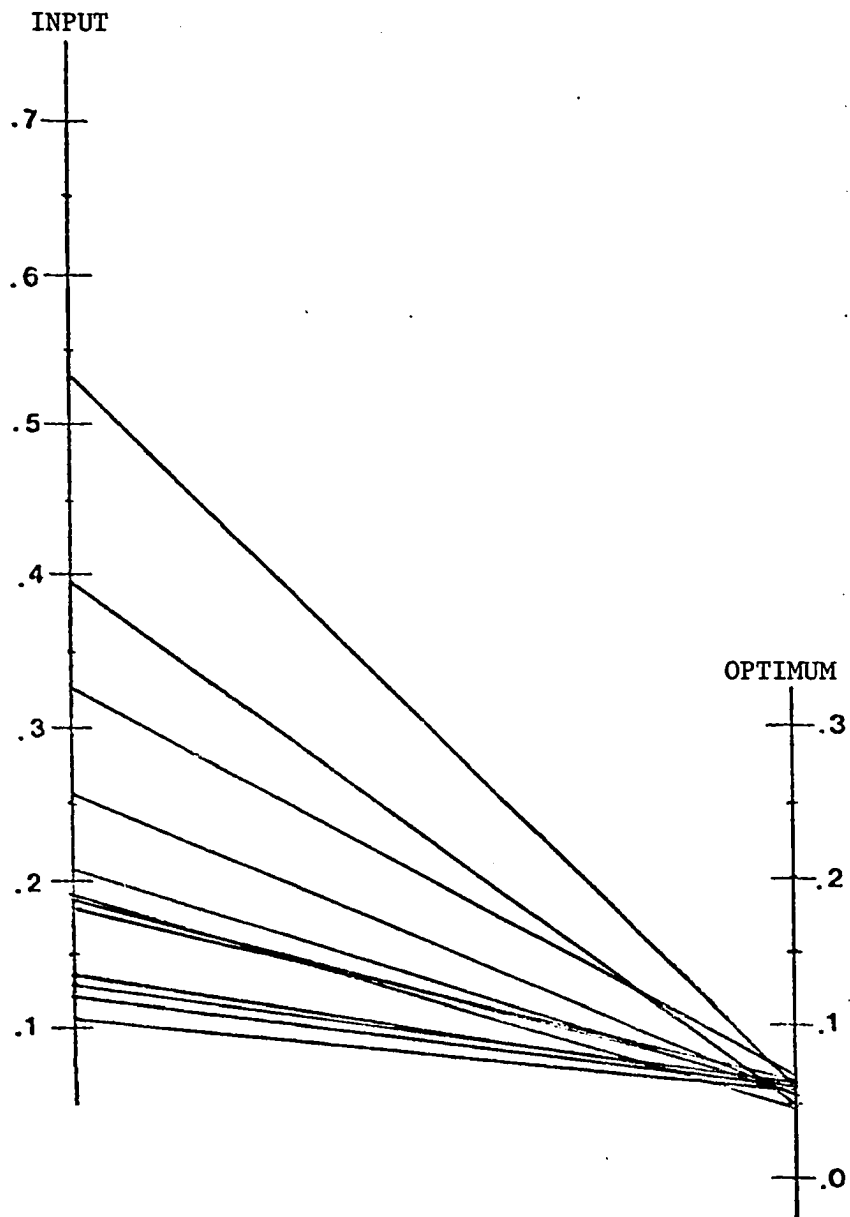


Figure 30: The objective function values for the input and optimum solution vectors for one signal function with $S/N = 100$.

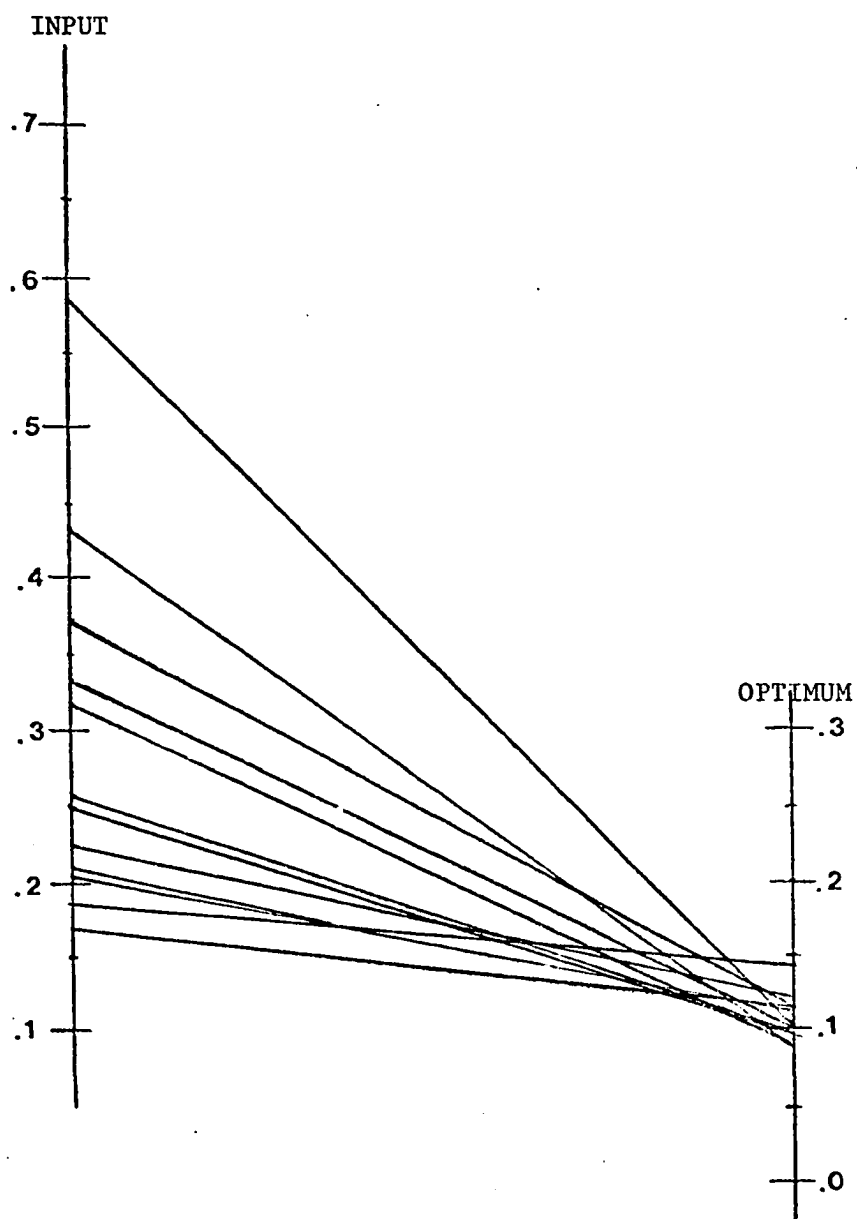


Figure 31: The objective function values for the input and optimum solution vectors for one signal function with $S/N = 10$.

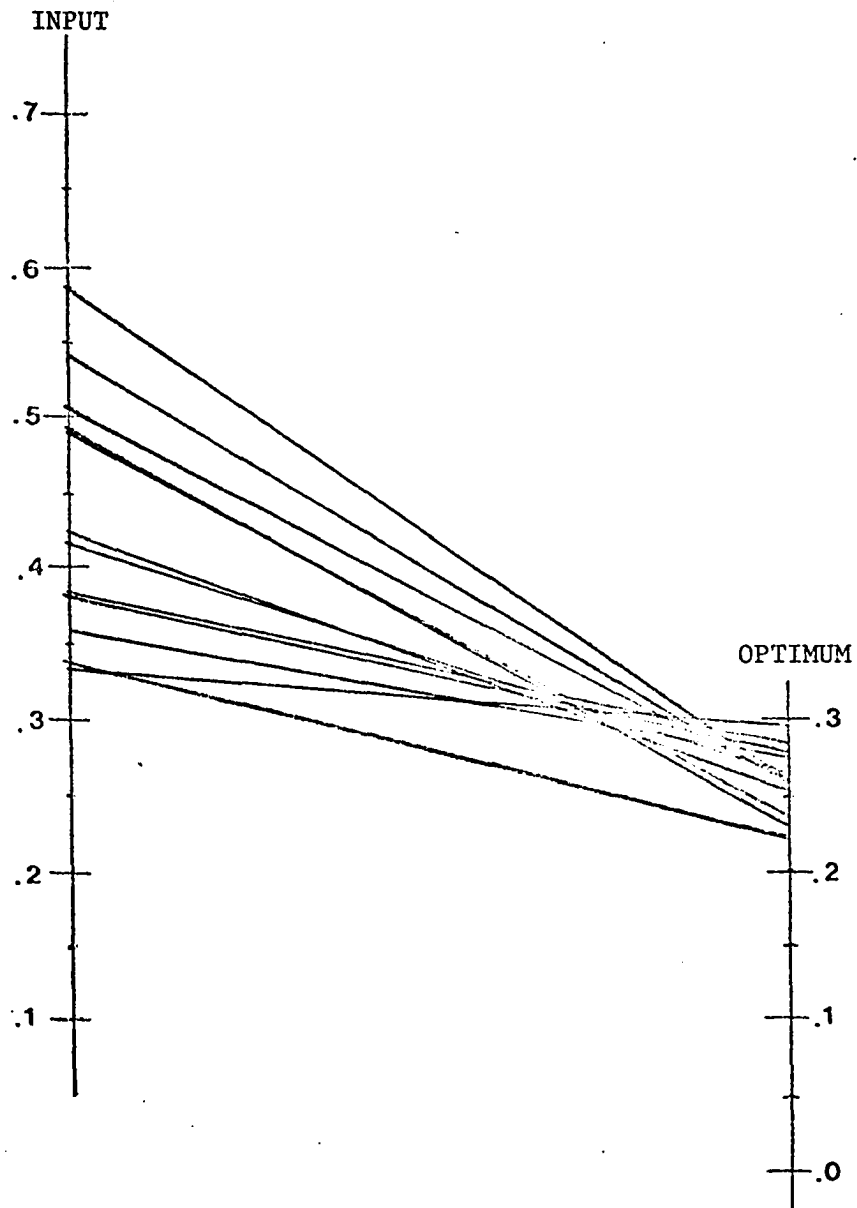


Figure 32: The objective function values for the input and optimum solution vectors for one signal function with $S/N = 1$.

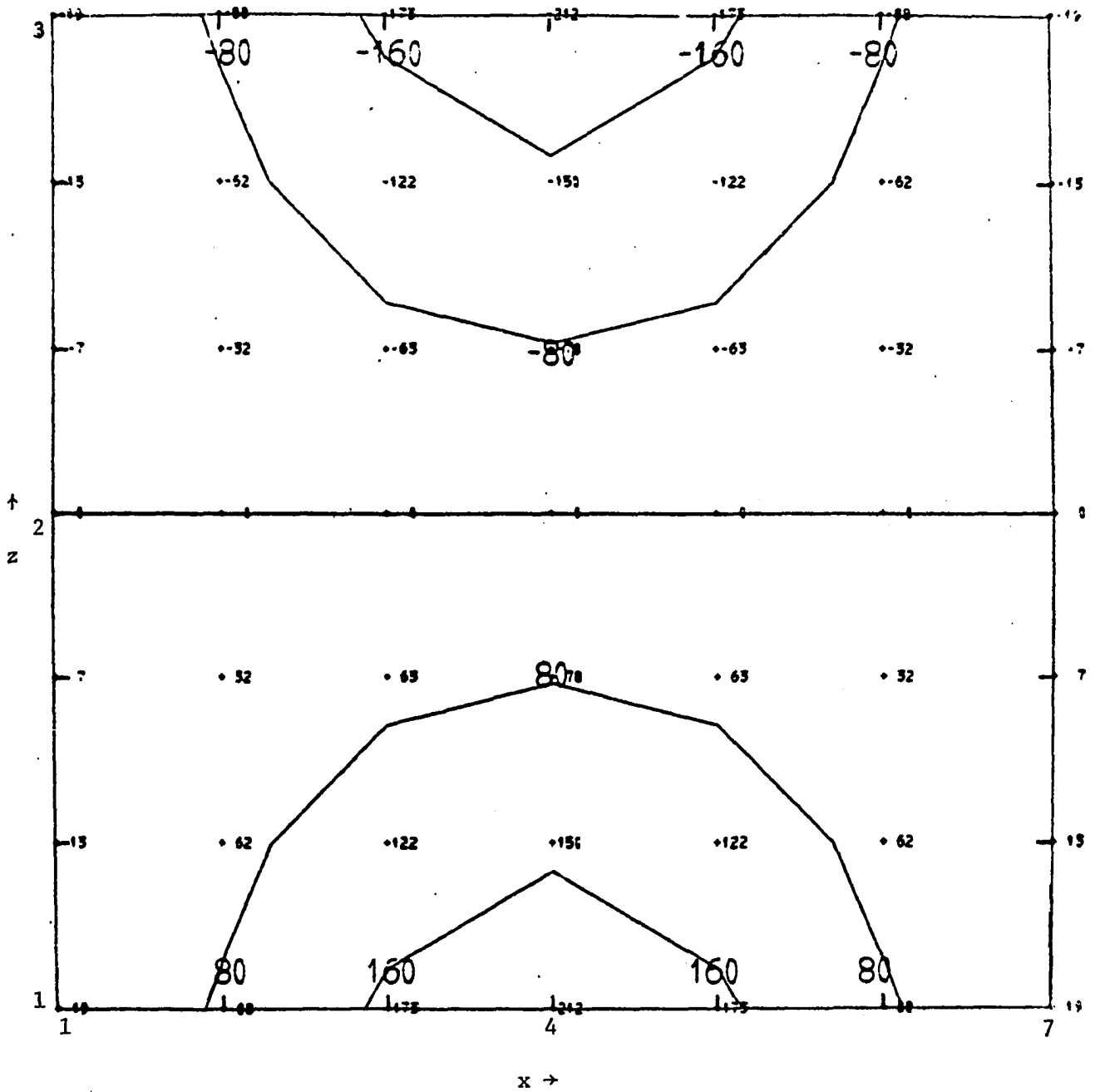


Figure 33: The true signal for all $y_i = 4$ displayed on a 7x7 grid where $1 \leq z \leq 3$. The maximum and minimum values on the grid are +212 and -212.

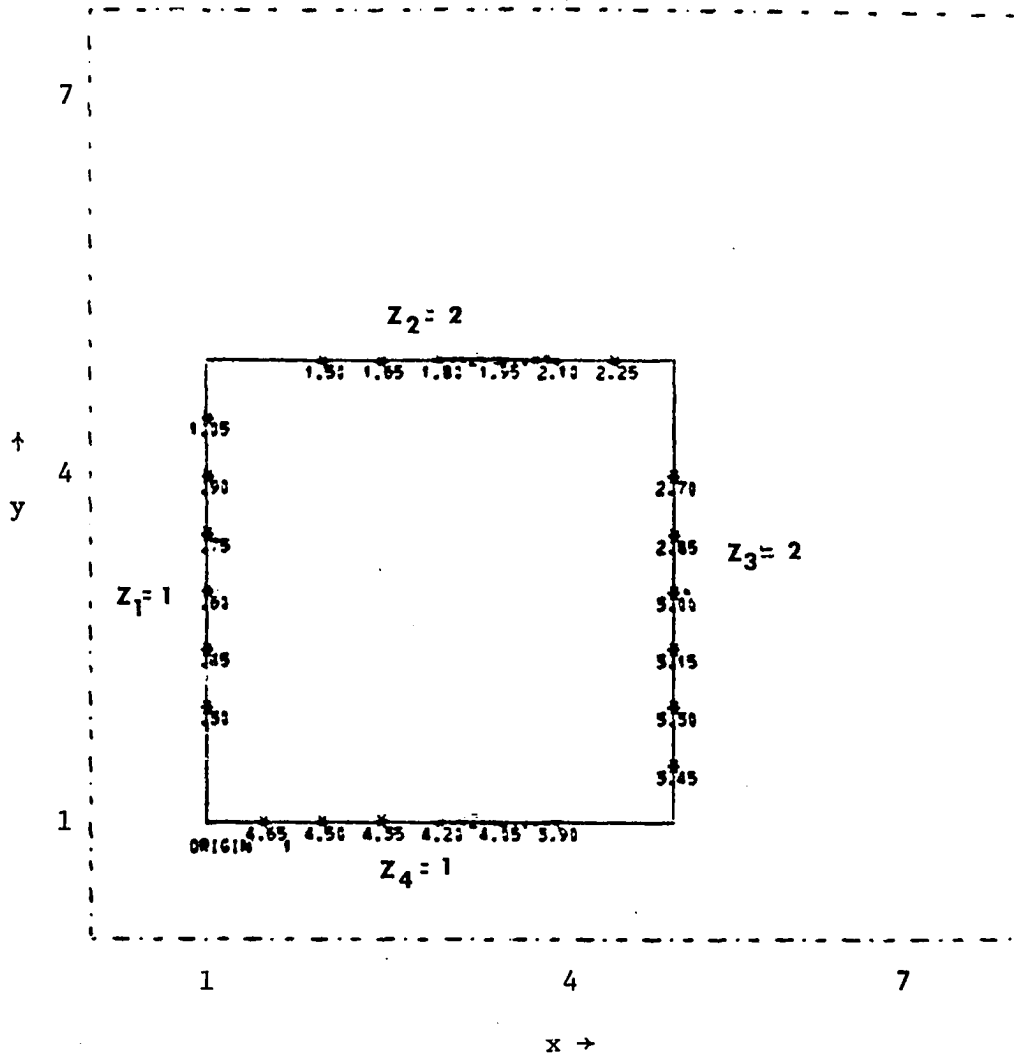


Figure 34: The sampling pattern used as input to the optimization algorithm in order to sample the signal shown in figures 4 through 6 in order to analyze the true signal (figure 33). All possible sample points are shown.

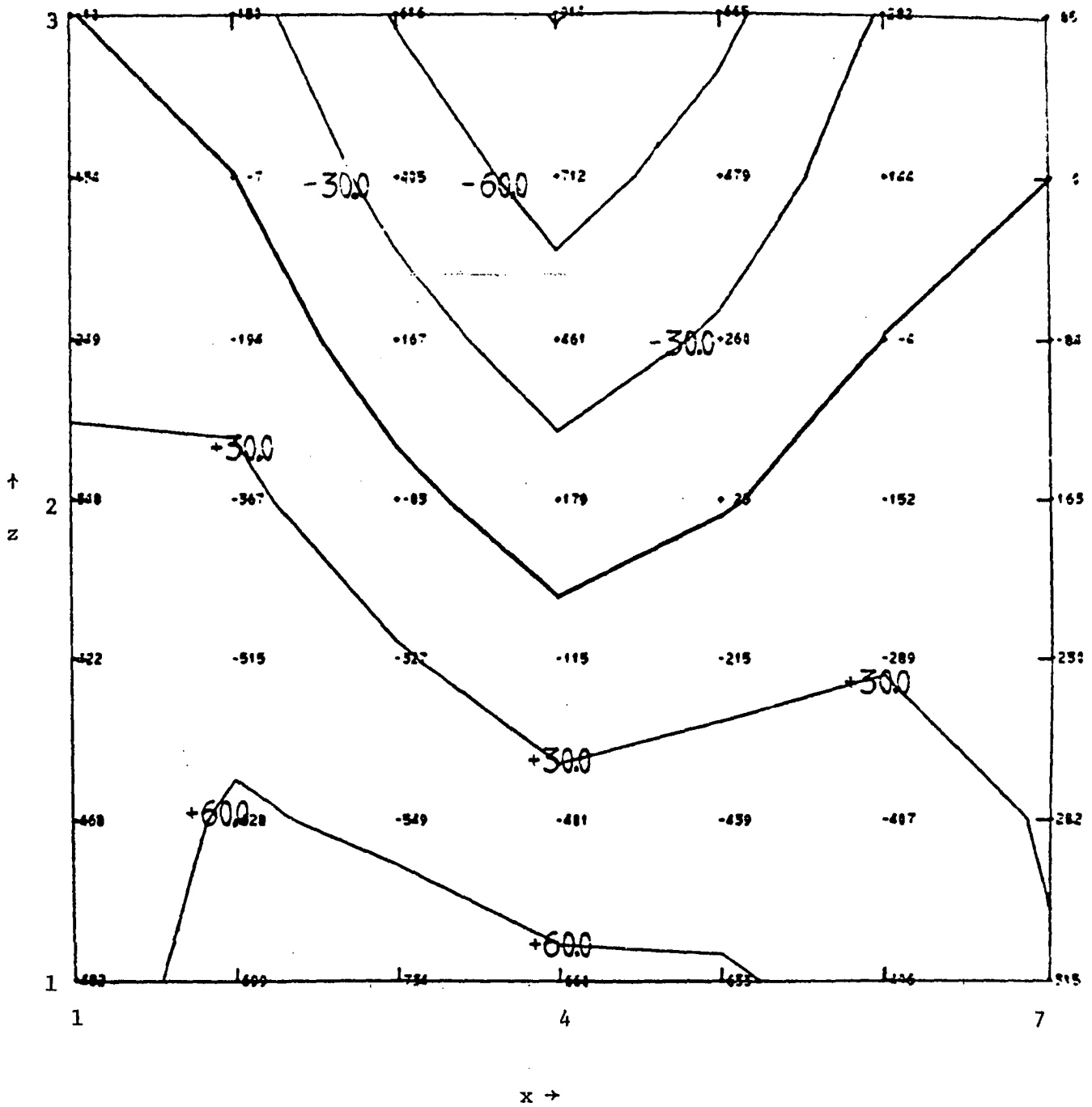


Figure 35: An objective analysis possible using the sample points of the input vector for $S/N = 1$. and $\rho_1 = 0$.

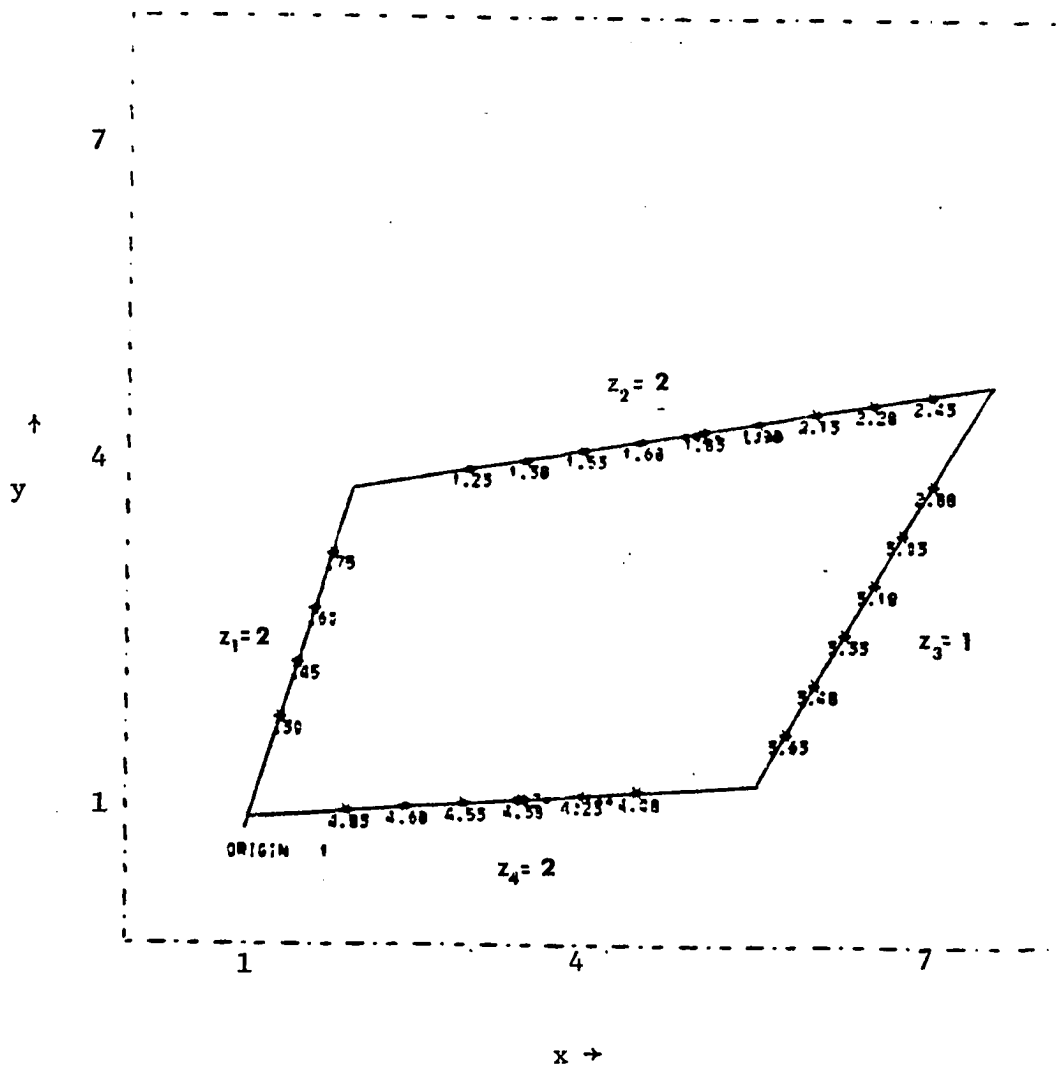


Figure 36: The optimal flight path and sampling locations computed by the optimization algorithm for an aircraft sampling in x, y, z, t .

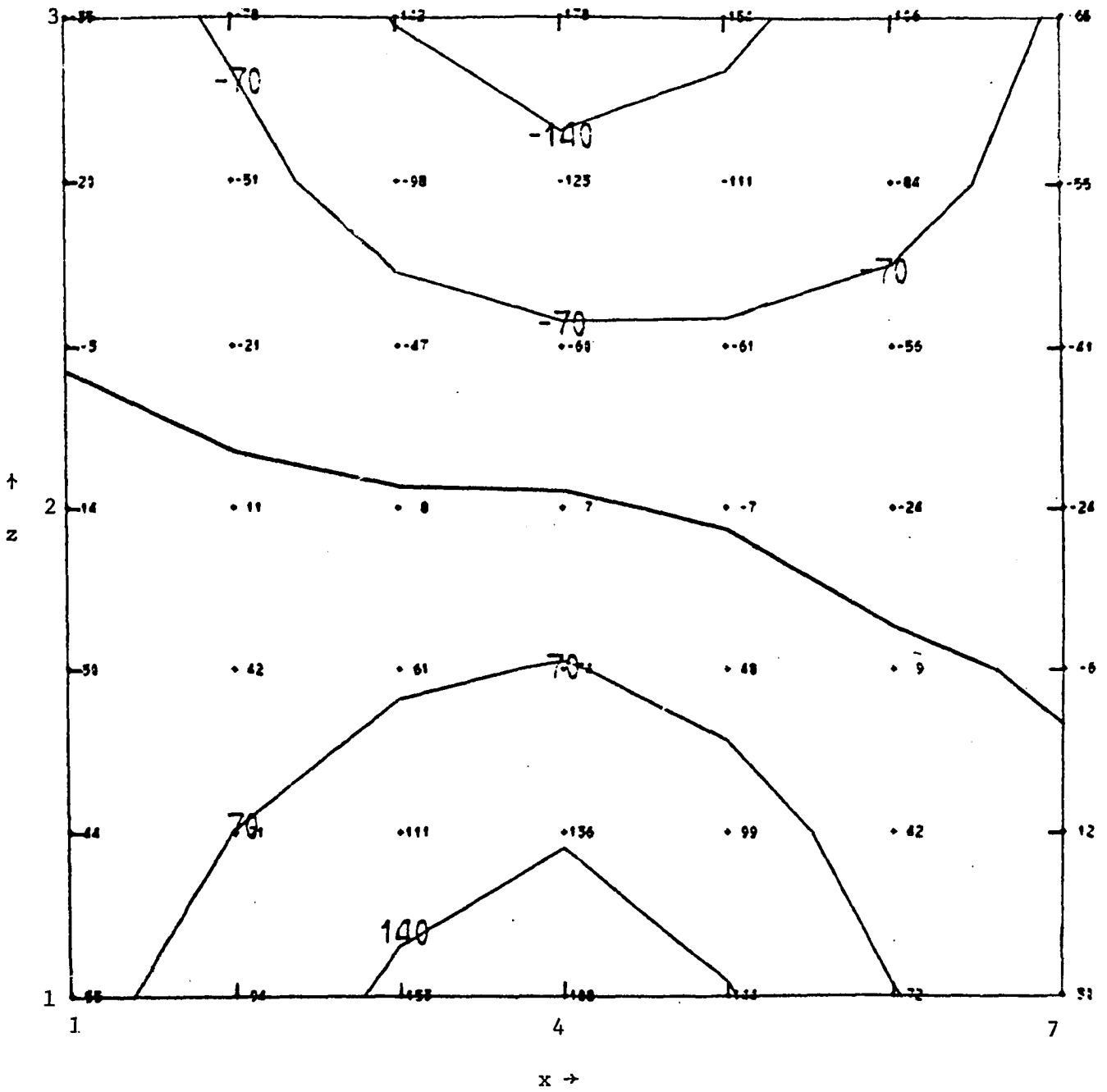


Figure 37: An objective analysis of the vertical shape of the true signal using the sample points available along the optimal path shown in figure 36 for $S/N = 1$. and $\rho_1 = 0$.

in an initial unexplained variance of .274 and an optimal amount of .157 . Many tests using this grid were run for different signal-to-noise ratios, different signal parameters and different input vectors. A movie has been produced on the NCAR CDC 6600/7600 computer system showing four different signal functions moving through a three-dimensional grid network with an aircraft flying an optimal flight track and sampling each system as it traverses the grid. Such a visual display is edifying, but hard to produce with figures in a paper.

Other tests have been conducted with this sampling scheme. They include sampling for a grid which extends throughout a space-time volume. The results of the objective analyses are difficult to display however. In addition to these tests, the signal origin and speeds were altered systematically in order to test the sensitivity of the optimal flight track derived from a single input vector.

Many other tests must be conducted in an effort to realize the usefulness of this optimal sampling methodology for planning field experiments. Many new applications of this sampling scheme are being planned. However, with just the results presented in this chapter, the potential of this optimal sampling scheme is obvious. This is especially true when one realizes the difficulty of aircraft flight planning compared with the placement of ground-based sensing systems.

CHAPTER VI

SUMMARY AND CONCLUSIONS

The optimal sampling and analysis methodology presented in this paper has taken advantage of recent developments in the fields of objective analysis and nonlinear programming along with the concepts of a multiple correlation coefficient and stepwise regression analysis. The goal has been to combine these techniques in order to achieve an objective solution to the problem of how to place sensors in a space-time volume in order to produce an optimal signal analysis. That goal has been achieved.

The elements of this methodology have remained relatively simple in an effort to make the optimal sampling scheme available for routine use by a wide range of experimenters. And, the methodology combines these elements in a modular fashion for ease in adapting the scheme to most types of sampling problems. That is, the variance-covariance relationships may take many analytic or empirical forms, any number of objective analysis techniques may be used, and the optimization algorithm may be changed to take advantage of the special form of the sampling problem.

Yet, despite the relative simplicity and modularity of this

optimal methodology, the results presented in this paper already are capable of providing some thoughts on the use of aircraft for field experiments. For instance, figures 15 through 22 indicate that flight planning with respect to a signal which evolves in x,y,z,t should be based upon temporal as well as spatial considerations. And, these same figures show that as the noise levels increase, the usefulness of the sampling is dramatically reduced even when the noise model is known. Without the noise model accurately defined, the use of observations (containing inseparable amounts of noise) in an objective analysis scheme could be disastrous. Therefore, at a minimum, a portion of data from each flight should be devoted to noise analysis.

Upon reviewing the objective analysis produced by the input vectors similar to figure 10, one might conclude that intuitive flight planning can have the same effect as increasing the noise level on the observations, i.e., decreasing the signal-to-noise ratio. The amount of effective decrease in signal-to-noise ratio is dependent on the skill of the flight planner. A part of the reason for the development of this methodology is to increase that skill for any experimenter without the expense in time and money of gaining the necessary experience by repeatedly conducting actual field experiments. Any number of "what if ..." 's may be tested through simulation to determine the relative importance of the variables in placing sensors in the sampling volume.

This optimal sampling and analysis methodology also has the

ability to test the feasibility of obtaining desired results for an experiment when the available resources are limited. Such an evaluation has been made using the Arctic High investigation mentioned previously with the conclusion that the resources were too limited to produce an acceptable signal analysis in the presence of a small signal-to-noise ratio. Similar feasibility studies could be conducted before every field exercise to determine the minimum resources which would be necessary before an experiment could be considered successful. Then, if at any time before the experiment, the resources were cut, the experiment could be cancelled.

Another reason for this methodology's development is to provide an operational tool in the field. Real time information could be given the optimization algorithm for the planning of each segment of a large experimental effort or for providing a strategy tree of actions to the experimenter. In fact, this application of the optimal sampling portion of the methodology could make use of the objectivity of the scheme. The day-to-day conduct of any field experiment might be able to be continued despite the physical or emotional health of one person.

This report only briefly shows the potential of this optimal sampling and analysis methodology. Many more tests and alterations will be necessary before the scheme can be applied to any one sampling problem. However, an approach is now available to answer the question of how to place sensors in a space-time volume in order to produce an optimal signal analysis when resources are restricted.

Peripheral developments in the areas of signal and noise analysis as well as in objective schemes to produce a posteriori information must continue in order that an entire systems approach to optimal experimental design (of which this optimal sampling and analysis is only a part) may be realized.

Further work with this basic sampling and analysis idea is being planned. First, an actual field experiment must be conducted using the methodology. And, the analysis results must be compared with other sampling methods. This test of the technique presented in this report must be done in conjunction with noise analysis techniques. It cannot be done without the effort and cooperation of competent individuals. It is for this reason that one idea for a field test might be to manage only a portion of an existing field exercise.

Other improvements to this methodology are being contemplated in an effort to make the optimal sampling ideas more general. One is a sequential updating plan which would attempt to define the signal covariance relationships when prior knowledge of the signal structure is unknown. Another is an overall management decision process which would provide a means of satisfying several goals for an experimental effort by selecting the particular goals to be attempted at any one time. Thus, the resources could be used optimally so that each goal could be attained during the experimental period.

Hopefully, this paper will stimulate the interests and ideas of those individuals who plan and conduct field experiments. Although not an answer to all the myriad problems associated with field

experiments, this optimal sampling and analysis methodology is capable of having a useful impact on increasing the probability of success.

LIST OF REFERENCES

- Alaka, M.A. and R.C. Elvander, 1972: "Matching of Observational Accuracy and Sampling Resolution in Meteorological Data Acquisition Experiments," Journal of Applied Meteorology, Vol. 11, #4, pp 567-577.
- Baer, L and G.W. Withee, 1971: "A Methodology for Defining Operational Synoptic Temporal Oceanic Sampling Systems. I. Stationary Conditions, II. Nonstationary Conditions," Journal of Applied Meteorology, Vol 10, #6, pp 1053-1065.
- Eddy, G.A., 1973: "The Objective Analysis of Atmospheric Structure," University of Oklahoma, Department of Meteorology report, submitted for publication.
- Eddy, G.A. and L. Rose, 1973: "A Cursory Look at the Effect of Wind Error on Kinematic Divergence," University of Oklahoma, Department of Meteorology report.
- Efroymsen, M.A., 1962: Mathematical Methods for Digital Computers, edited by A. Ralston and H.S. Wilf, J. Wiley and Sons, pp 191-199.
- Gandin, L.S., S.A. Mashkovich, M.A. Alaka and F.M. Lewis, 1967: Design of Optimum Networks for Aerological Observing Stations. World Weather Watch Planning Report #21, WMO, Geneva, Switzerland.
- Himmelblau, D.M., 1972: Applied Nonlinear Programming, McGraw-Hill, Inc, New York.
- Kasahara, A., 1972: "Simulation Experiments for Meteorological Observing Systems for GARP," Bulletin of the American Meteorological Society, Vol 53, #3, pp 252-264.
- Kays, M.D., 1973: personal communication.
- Lacy, C., 1973: "Objective Analysis using Modelled Space-Time Covariances: An Evaluation," received at the Atmospheric Sciences Laboratory, White Sands Missile Range, N.M., submitted for publication.

- Northrup, G.M., E.L. Davis and E.R. Sweeton, 1972: Environmental Models/Systems Effectiveness Study (EM/SE). Center for Environment and Man, #4052-436.
- Reinelt, E.R., 1973: "On the Synoptic Climatology of Migrant Arctic Highs on the Great Plains," University of Oklahoma, Department of Meteorology report.
- Yerg, M.C., 1973: "A Systems Approach to Optimal Experimental Design in Meteorology," University of Oklahoma, Department of Meteorology report.
- Zipser, E., 1973: a second draft of "A Proposed Aircraft Plan for the GARP Atlantic Tropical Experiment (GATE)," National Center for Atmospheric Research, Boulder, Colorado.